International Journal of Environmental Science and Technology
https://doi.org/10.1007/s13762-024-06319-8

ORIGINAL PAPER

Biorefinery practice for valorizing Mediterranean bloomed *Pterocladia capillacea* into valued and sustainable bioproducts with numerous green solicitations

N. Sh. El-Gendy[1,2] · H. N. Nassar[1,2,3] · A. R. Ismail[1] · H. R. Ali[1] · B. A. Ali[4] · K. M. Abdelsalam[5] · M. Mubarak[6]

Received: 12 July 2024 / Revised: 21 November 2024 / Accepted: 30 December 2024

Abstract

As a solution for ecosystem bioremediation from the gigantic red seaweed proliferation across the Mediterranean shorelines, this work investigates the effective utilization of *Pterocladia capillacea* to produce different esteemed and viable bioproducts. The nutritional composition of approximately 6.88 ± 0.31%, 20.15 ± 0.2%, 42.16 ± 0.3%, and 2.51 ± 0.05% (w:w) protein, fiber, carbohydrate, and lipid, respectively, promotes its application in the human food and animal fodder industries. Its $N + P_2O_5 + K_2O$, undesirable heavy metals, organic carbon, and organic matter contents of 5.48 ± 0.07%, 2.82 ± 0.15 mg/kg, 16.11 ± 0.15%, and 27.71 ± 0.26% are all within the ranges allowed by the Egyptian standard for organic fertilizer. Its calorific value of 16.16 ± 0.5 MJ/kg and relatively low ash and heavy metals contents are in accordance with the international standards for primary solid biofuel. Its relatively high holocellulose content of 44 ± 0.5% (w/w) recommends its applicability in the liquid biofuels sector. Further, via a pioneering practice, a sequential, eco-friendly, and fully integrated bioprocess *Pt. capillacea* biomass is valorized into natural pigments of approximately 5.05 ± 0.05 mg/g total chlorophyll, 2.12 ± 0.05 mg/g carotenoids, phycobiliproteins of approximately 1.33 ± 0.05 mg/g phycocyanin, 3.07 ± 0.05 mg/g allophycocyanin, and 0.97 ± 0.05 mg/g phycoerythrin, hydrocolloids of approximately 28.21 ± 2.5% carrageenan and 20.46 ± 1.5% agar, and finally cellulose of approximately 20.15 ± 1.5%. Additionally, the extracted carrageenan proved an efficient antimicrobial action against pathogenic microorganisms that supports its use for water densification, food packing, and wound dressing.

Keywords *Pterocladia capillacea* valorization · Fully integrated biorefinery process · Value-added products · Blue economy

Editorial responsibility: Samareh Mirkia.

✉ N. Sh. El-Gendy
nourepri@yahoo.com

1 Egyptian Petroleum Research Institute (EPRI), Nasr City, Cairo 11727, Egypt

2 Center of Excellence, October University for Modern Sciences and Arts (MSA), 6th of October City, Giza 12566, Egypt

3 Faculty of Physical Therapy, October University for Modern Sciences and Arts (MSA), 6th of October City, Giza 12566, Egypt

4 General Organization for Export and Import Control (GOEIC), Cairo, Egypt

5 Marine Environment Division, National Institute of Oceanography and Fisheries NIOF, Alexandria Branch, Alexanderia 21519, Egypt

6 Soil and Water Department, Faculty of Agriculture, Ain Shamas University, Cairo 11241, Egypt

Introduction

Red seaweed is known to be commercially significant, accounting for about 61% of the total worldwide seaweed yield (Álvarez-Viñas et al. 2019). Along the Mediterranean coast of Egypt, particularly near Alexandria, vast arrays of seaweed thrive. One of the most prevalent macroalgae on the shore of Alexandria is *Pterocladia capillacea*, which is especially plentiful from spring until autumn (Khairy and El-Shafay 2013; Hassaan et al. 2021; Al-Saeedi et al. 2023). It typically inhabits shallow water and rocks close to the coast in the Alexandria Mediterranean Sea (Ashour et al. 2020). For a variety of marine inhabitants, including fish, turtles, and prawns, the presence of macroalgae in an eco-balanced amount with a regular rate of growth is advantageous since it can give food, oxygen, and a place to reside (Wang et al. 2020a). However, the proliferation of seaweed is seen as an environmental peril and a threat to the ecology (Abu Hafsa

Published online: 04 March 2025

et al. 2021). Globally, quicker nutrient uptake, faster growth, and more frequent macroalgal blooms have resulted from the expansion of human population, fertilizer use, animal waste production, and fossil fuel burning, which have surmounted the nitrogen and phosphorus restriction of coastal and estuary waters (El Shoubaky 2013). In addition to eutrophication, herbivory loss, inadequate water reddening, and low tide activity, climate changes also cause macroalgal blooms through elevated irradiation, temperature, and seawater acidification (Lyons et al. 2012). Given their capacity to absorb pollutants (such as trace metals), macroalgae can serve as markers of both pollution and eutrophication in ecological assessments (Gubelit 2022). Increased levels of nutrients and organic pollutants from aquaculture, agriculture, domestic, and industrial activities mostly cause harmful macroalgal blooms (Joniver et al. 2021). Although they can exist in tropical and temperate regions, shallow coastal waters and fruitful estuaries are more frequently home to them (Lyons et al. 2014).

The negative effects of macroalgal blooms on the environment, economy, and society are numerous. Macroalgal proliferation and blooms reduce light penetration, water clarity, and deplete oxygen. As a result, they adversely impact various aspects such as ecology, biological composition, zoobenthic communities, seagrass, marine biodiversity, life beneath the water, and the food chain (Lane-Medeiros et al. 2023). It increases the occurrence of biofouling and microbial influenced corrosion, negatively affecting infrastructure, maritime, and industrial activities (Lapointe et al. 2018). Macroalgal blooms impede tourism, fishing, mariculture, and recreational activities while also detracting from the aesthetic appeal of the coastal zone (El-Gendy et al. 2023). Rotten macroalgal mats release harmful gases that negatively affect human wellbeing (Wang et al. 2020a). Usually, the overgrowth of the red seaweed *Pt. capillacea* obstructs fishing activities in the Alexandria Mediterranean shoreline, as it gathers within fishing nets, thereby decreasing the fishing yield. Moreover, the blooming of red seaweed, would secret some toxins, and would also be followed by the biomass decay and degradation, which emits the toxic and corrosive sulfides (for example, carbon disulfide, hydrogen sulfide, and methyl sulfide), accumulates carbon dioxide, increases water acidity, depletes dissolved oxygen, and consequently negatively impacted the water quality and life underneath water (Young et al. 2022). Thus, would lead to the fish, bivalve, and benthic organism mortality, in addition to costly cleaning undertakings, and a decline in touristic activities (Lyons et al. 2014; Joniver et al. 2021). Not only that, but the overgrowth of red seaweed in some coastal zones has also been reported to negatively impacts coral reefs (Arasamuthu et al. 2023) and other communal occupants of the littoral region (Eklund et al. 2005), especially upon their death and decay. These negative consequences have raised a tremendous deal of worry and necessitated expensive programs to confiscate such blooms from the afflicted areas.

A lot of interest has recently been shown in the valorization of such wasteful macroalgal biomass, especially the red seaweed, into various value-added products and sustainable biopolymers due to their numerous applications in the food, pharmaceutical, fertilizers, biofuels, dyes, biodegradable plastics, and animal feeder sectors (Lapointe et al. 2018; Torres et al. 2019; Castejón et al. 2021; Guillén et al. 2022; Nallasivam et al. 2022; Martins et al. 2023). Developing and implementing biomass treatment strategies that enable us to recover as much of the useful components in the red seaweed biomass as is feasible is crucial from the perspective of a biorefinery. Such methods, as opposed to a conventional "single-compound" strategy, would aid in reducing greenhouse gas (GHG) emissions and the buildup of waste fractions from industrial production. The main industrial and mature technology is the production of agar and carrageenan from agarophyte and carrageenophyte red seaweed, respectively (Baghel 2023). The *Pt. capillacea* has been published for valuable single-compound production, for example, agar (Rao and Bekheet 1976; Freile-Pelegrín et al. 1996; Lai and Lii 1998; 2002; Fathy and Mohammady 2007; Mayhoob et al. 2017)**.** Researchers have also used *Pterocladia* species as a carrageenan source (Sebaaly et al. 2012), while Siddhanta et al. (2013) reported using *Pt. heteroplatos* for cellulose production. Despite the lavishness of *Pt. capillacea* along the Mediterranean coast, to our knowledge, there is no published research explores the valuation of *Pt. capillacea* into different value-added products via a sequential, fully integrated eco-friendly process.

This work aims to collect and characterize one of the most abundant red seaweed, *Pt. capillacea*, which inhabits the Egyptian Mediterranean coast. For its promotion in the blue-economy instead of being an environmental issue, this work also targets exploring the primary biochemical components of collected *Pt. capillacea* as well as its proximate and mineral composition to suggest its possible industrial applications. Moreover, the primary objective of this manuscript is to develop in a pioneer step a fully integrated process to sequentially extract valuable natural pigments and biopolymers (carrageenan, agar, and cellulose). Thus, briefly, the aim is to efficiently utilize the entire biomass of *Pt. capillacea*, maximize its value chain, and steer clear of the existing conventional industrial approach that extracts a "single compound" and leaves behind significant quantities of wasted, unused biomass.

Materials and methods

Seaweed collection and preparation

The red seaweed was harvested during late summer and early autumn 2023 from Abu-Qir Bay in Alexandria, Egypt

(31°18'44.5"N 30°02′40.2"E). It was easily collected manually from the submerged rocks and from fishermen, as it is usually collected in fishing nets during fishing activities. At the National Institute of Oceanography and Fisheries (NIOF), Alexandria Branch, Egypt, the collected red seaweed was examined microscopically in accordance with Iha et al. (2017) and Wang et al. (2020b). That has been performed using a stereo microscope (Novex, model P-20, EUROMEX microscopes BV, Arnheim, the Netherlands) and a light microscope (Optika model B-192, S.r.l.Via Rigla, Ponteranica (BG), Italy).

To remove salt, undesirable sand, and other debris, the harvested seaweed was rinsed with tap water. They were then left to dry in the sun. These were then ground and sieved to create a homogenous 0.8–1 mm solid biomass. Ultimately, they were stored in sterile, sealed plastic bags until needed.

The biomass analysis of the collected red seaweed

The Soil and Water Unit (SWU), Central Lab, Faculty of Agricultural, Ain Shams University, Egypt, determined the nutritional composition of the harvested red seaweed using the methods outlined in AOAC (2000). The General Organization for Export and Import Control (GOEIC), Egypt, conducted the proximate analysis. This required the use of standard methodologies such as ASTM D5865-2019, EN15402-2011, EN15403-2011, and EN15414-2011 to measure the calorific value, volatile matter, ash, and moisture contents, respectively. The quantities of cellulose, hemicellulose, and lignin have been measured using the technique as reported by Moubasher et al. (1984). The SWU has performed other physico- and bio-chemical analyses in accordance with El-Gendy et al. (2023). The organic carbon and matter have been determined using the Walkley and Black (1934) method. The electrical conductivity and pH have been measured using the Jackson (1973) approach. The Kjeldahl digestion method, as described by Chapman and Pratt (1961), has been used to measure the total N-content. The crude protein concentration has been computed by multiplying the value by 6.25, which served as a conversion factor. Total phosphorus has been measured using the protocol described by Watanabe and Olsen (1965). The remaining minerals and heavy metals have been measured using the methodology described by Benton (2001). That has been performed using ICP-MS (inductively coupled plasma mass spectrometry, Spectro Ciros CCD ICP-OES, Spectro Analytical Instruments, Kleve, Germany).

A fully integrated method for extracting value-added products from the harvested red seaweed

The consecutive, fully integrated process used to extract various value-added products from the harvested red seaweed is illustrated in Fig. 1. Twenty-five grams of the ground algal biomass were soaked in 500 mL acetone:ethanol (1:1 v/v) and heated under reflux at 60 °C for 1 h for the extraction of hydrophobic and hydrophilic pigments (Sebaaly et al. 2012). Next, filtration via a cotton mesh cloth separated the residual biomass, and a rotary evaporator set at 40 °C recovered the solvent (Fig. 1). For the carrageenan extraction, the obtained residual biomass was then soaked into a 2 M NaOH solution (1:20 w/V) and heated in a water bath set at 70 °C for 1 h (Han et al. 2021). The mixture was then filtered through a cotton mesh cloth to separate the residual algal biomass for the subsequent agar extraction according to a modified method reported by Ibrahim et al. (2015). The carrageenan was precipitated in the obtained filtrate by adding excess 95% ethanol (1:2 v/v filtrate/ethanol). The obtained precipitate was decanted and dried overnight at room temperature and then grinded to obtain the carrageenan powder. The biomass residue was then hydrothermally treated by soaking in distilled water (1:20 w/v) and then autoclaving at 121 °C and 1 bar for 20 min (Fig. 1). The mixture was then filtered through a cotton mesh cloth to separate the residual algal biomass for the subsequent cellulose extraction in accordance with the method reported by El-Gendy et al. (2023), as illustrated in Fig. 1. The obtained filtrate was assembled into trays and left overnight at −20 °C to gel. After thawing, the gel was twice cleaned with 20 mL distilled water, allowed to dry overnight at room temperature, and then grinded to obtain the agar powder (Fig. 1). Results were provided in the form of mean and ± standard deviation based on triple experiments.

Analysis of the extracted value-added products

According to Ismail (2016), an ultraviolet/visible/near infrared (UV/Vis/NIR) double beam spectrophotometer (model V-570, JASCO International Co., Ltd., Tokyo, Japan) was used to identify the extracted mixture of pigments and anti-oxidants. The wavelength range of 190–800 nm was scanned for the distinctive absorption spectra (Haryatfrehni et al. 2015).

The extracted chlorophylls and carotenoids were calculated in accordance with Ismail (2016) as follows;

$$\text{Chloropyll}_a(\text{mg/g}) = \frac{\left[12.7\text{A}_{663} - 2.69\text{A}_{645}\right] \times \text{V}}{\text{W}} \quad (1)$$

$$\text{Total Chloropyll (mg/g)} = \frac{\left[20.2A_{645} + 8.02A_{663}\right] \times V}{W} \quad (2)$$

$$\text{Carotenoids (mg/g)} = \frac{4A_{480} \times V}{W} \quad (3)$$

$$\beta - Carotene(mg/g) = \frac{[0.216 \times A_{663} - 0.304 \times A_{450} + 0.452 \times A_{453}] \times \text{V}}{W} \quad (4)$$

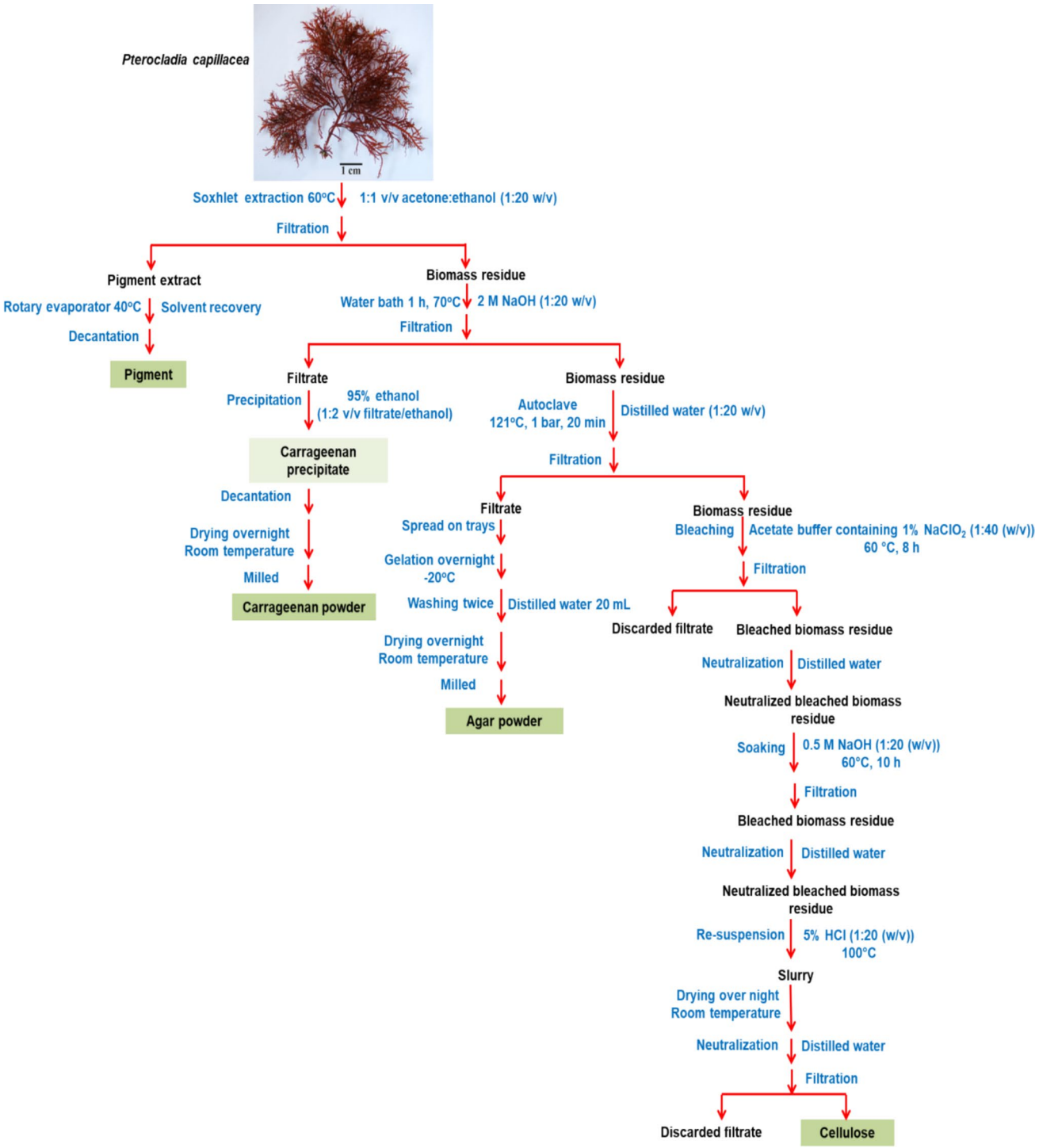

Fig. 1 A sequential, fully integrated method for producing valued bioproducts from the collected *Pterocladia capillacea*

The phycobiliproteins (i.e. phycoerythrins, phycocyanin, and allophycocyanin) concentration was calculated according to Ismail and Osman (2016);

$$Phycocyanin(mg/g) = \frac{A_{615} \times 0.457A_{652}}{5.34} \quad (5)$$

$$Allophycocyanin(mg/g) = \frac{A_{652} - 0.208A_{615}}{5.09} \quad (6)$$

$$Phycoerythrin(mg/g) = \frac{A_{562} - (2.41 phycocyanin) - (0.849 allophycocyanin)}{9.62} \quad (7)$$

The other extracted value-added products were characterized in accordance with El-Gendy et al. (2023). Using the KBr disc approach, the Fourier transform infrared (FTIR, Perkin Elmer Spectrum One, Waltham, MA, USA) was used to determine the characteristic functional groups of value-added products. The spectra were scanned at a rate of 16 cm/min, achieving a scan resolution of 4 cm^{-1} within the 400–4000 cm^{-1} range. A high-resolution X-ray diffractometer (XRD, PANalytical XPERT PRO MPD, Lelyweg, EA Almelo, the Netherlands) with a Cu k_{α} radiation source ($\lambda = 1.5418$ Å) working at 40 kV and 40 mA was used to determine the XRD patterns of the extracted value-added products. A dynamic light scattering device (DLS, ZetaSizer Nano Series (HT), Nano ZS, Malvern Instruments, Malvern, UK) was used to evaluate the average particle size. A field emission scanning electron microscope equipped with smart energy dispersive X-ray spectroscopy (FESEM-EDX, model Sigma 300VP Carl Zeiss, Jena, Germany) was used to study the granule shape of the extracted value-added products. A field emission scanning electron microscope with smart energy dispersive X-ray spectroscopy (FESEM-EDX; model Sigma 300VP; Carl Zeiss, Jena, Germany) was applied to examine the granular morphology. Furthermore, the thermal characteristics of the value-added products were examined under nitrogen conditions using Q600 SDT simultaneous differential scanning calorimetry-thermal gravimetric analysis (DSC–TGA) and the TA instrument Discovery DSC250 (New Castle, DE, USA) to produce their DSC data, respectively. Utilizing TA Instruments Trios software (V5.2.2.47561, New Castle, DE, USA), the acquired thermograms were analyzed. The gelatinization enthalpy (ΔH J/g) was then computed by dividing the integrated peak area by the weight of the value-added product slurry (5 mg) and the heating temperature rate (5 °C/min).

Antimicrobial activity of extract carrageenan

The antimicrobial activity of the extracted *Pt. capillacea* carrageenan was also evaluated against some pathogenic bacteria and yeast using the standard disk diffusion protocol as reported by Ismail and Amer (2020). Tryptone glucose yeast agar (TGY-agar) plates were employed (Nassar et al. 2022) and 5 mm disk supplemented with 5 mg/L carrageenan was used. The tested Gram negative bacteria were *Pseudomonas putida* ATCC 10145 and *Escherichia coli* ATCC 23282, while the Gram positive ones were *Staphylococcus aureus* ATCC 35556 and *Bacillus subtilis* ATCC 6633, the tested yeast was *Candida albicans* IMRU 3669, and the tested fungal strain was *Aspergillus niger* ATCC 16404. Standard antimicrobial agents were employed as positive controls, with streptomycin (50 µg/mL) as an antibacterial and metronidazole (100 µg/mL) as an anti-yeast and anti-fungal. All plates were incubated at 30°C, those inoculated with bacteria and yeast for 48 h, while those inoculated with fungi for 7 days.

The activity index of the extracted carrageenan was computed depending on the size of the inhibitory zone (mm), using the following equation (El-Gendy et al. 2023):

$$Activity\ index = \frac{Carrageenan\ inhibition\ zone\ (mm)}{Standard\ antibiotic\ inhibition\ zone\ (mm)} \quad (8)$$

To establish the significance difference between the acquired data, a Tukey-test was done using SPSS software version 13.0 (Informer Technologies, Inc., Los Angeles, CA, USA), with p values greater than 0.05 considered non-significant at the 95% confidence level.

To ensure reproducibility, each analysis was carried out three times, and the mean data were presented as average mean values ± standard deviation (StD), with a 95% confidence level.

Results and discussion

An examination of the morphology of the harvested red seaweed

The visual (Fig. 2) and stereomicroscopic (Supplementary Fig. 1) examination of the collected red seaweed bore a striking resemblance to *Pterocladia capillacea*, a member of the phylum Rhodophyta, class Florideophyceae, order Gelidiales, and family Pterocladiaceae. It frequently grows on rocks in the shallow subtidal and lower intertidal zones. *Pt. pyramidale* is its other popular name. The visual observation of *Pt. capillacea* habit (Fig. 2) aligns with that reported by Ismail and Osman (2016), Ismail et al. (2020), and Abou Gabal et al. (2021). Ibrahim et al. (2015) and Rashad and El-Chaghaby (2020) have reported that the most prevalent agarophyte growing around the shoreline of Alexandria, especially in Abu-Qir, is the Rhodophyta *Pt. capillacea*. Shams El-Dinet al. (2015) have also reported the abundance of *Pt. capillacea* in the Mediterranean Alexandria shoreline.

The visual observation (Fig. 2) reveals a dark reddish-purple to reddish-wine colored plant that bears a striking resemblance to feathers. Its fronds are flat and cartilaginous. Its thallus can reach a height of approximately 10 cm, and its distichous branching is regular (Fig. 2b). Figure 2 shows distal portions of the primary axis and lateral branches grow into terete axes that curve downward

and reconnect with the substrate substratum, making secondary prostrate axes. The main axis is cylindrical below and flattened above and the order of branching reaches up to four orders. The thalli sometimes look like a Christmas tree (Fig. 2b), and sometimes its outline is clearly pyramidal or triangular in shape (Fig. 2e). Boo et al. (2010) reported a similar observation. The variation in thallus morphology, between being regularly pinnate, with numerous, short and closely packed lateral branches (Fig. 2a, b) and irregular branching (Fig. 2) has been previously reported by Bottalico et al. (2008) and related that to the age of the seaweed. It is pinnate or bipinnate (Fig. 2b–e), but naked at the base (Fig. 2a). It has oppositely tapering branches (Fig. 2a). From a rhizoidal base, loose tufts of fronds emerge (Fig. 2c). The holdfast, which harbors peg-like haptera on its stolons (arrows in Fig. 2a, b) was also observed by Wang et al. (2020b). The different degree in branch development concerning the fronds with and without a main apex (Fig. 2) coincides with what is reported by Scrosati (2002). Different cross-sections of *Pt. capillacea* have also been microscopically examined. The microscopic examination at different magnification powers (Supplementary Figs. 1–3) matched well with what have been previously reported by Boo et al. (2010), Iha et al. (2017), Patarra et al. (2020), and Wang et al. (2020b). The stereo-microscopic examination (Supplementary Figs. 1–3) proved the presence of the three reproductive types; tetrasporophytes, beside the female and male gametophytes. A similar observation was reported by Wang et al. (2020b).

The biomass analysis of the collected *Pterocladia capillacea*

Seaweed have varying nutritional contents based on their species, habitats, age, surrounding conditions, harvesting season, and geographic location (Wu et al. 2014; Doh et al. 2020). However, the results of nutritional analysis of the collected *Pt. capillacea* of 6.89 ± 0.31, 20.15 ± 0.2, 42.16 ± 0.3, 2.51 ± 0.05, and $17.4 \pm 0.5\%$ (w/w) protein, fiber, carbohydrate, lipid, and ash, respectively (Table 1) are found to match well with those reported for red seaweed (Øverland et al. 2019). This also aligns with the nutritional analysis of *Pt. capillacea* that Khairy and El-Shafay (2013) collected from Abu-Qir Bay. The lipid, carbohydrates, proteins, ash, and fiber content in red seaweed can range between 0–3%, 4.3–77%, 2–50%, 2–39%, and 5.7–64.7%, respectively (Gamero-Vega et al. 2020; Zhou et al. 2022; Baghel 2023). It was found that the ash content was about $17.4 \pm 0.5\%$ (w/w, Table 1). This is higher than what was found in a study of *Pt. capillacea* collected from the Mediterranean coast of Alexandria, Egypt, in 2022, which was 15.78% (w:w) (Shoaib et al. 2022). The tabulated relatively high concentrations of carbohydrates and protein in *Pt. capillacea* biomass (Table 1) have also been reported for red seaweed collected from Alexandria shorelines (Rashad and El-Chaghaby 2020). The abundance of the carbohydrate content in *Pt. capillacea* biomass (Table 1) has been previously reported by Wu et al. (2014). The lipid content of approximately 2.51 ± 0.05 wt% (w/w, Table 1) is in accordance with that reported by Wassef et al. (2013) and Ashour et al. (2020). It is worth to mention that the fiber content of the collected *Pt. capillacea* was higher than that of the green

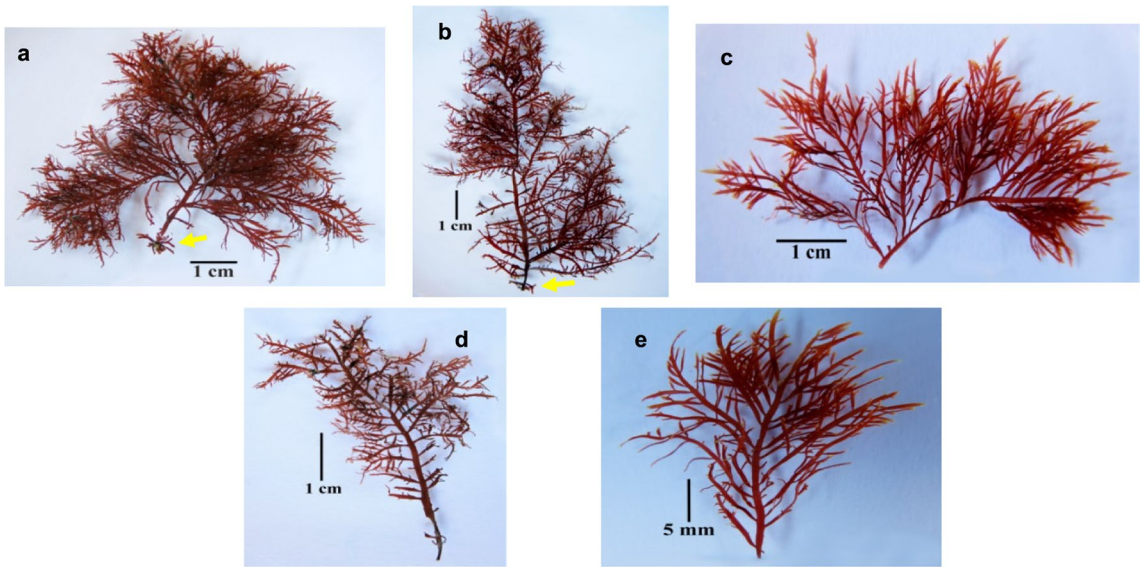

Fig. 2 Pterocladia capillacea

Ulva fasciata that we have previously collected from Alexandria shorelines (El-Gendy et al. 2023), which recorded 9.9% (w/w). However, the carbohydrate and lipid contents were comparable, which recorded approximately 44.85% and 3.27% in green *U. fasciata*, respectively (El-Gendy et al. 2023). That encouraged on working on both of the collected red *Pt. capillacea* and green *U. fasciata* to study their potentiality on animal feed industry.

The tabulated concentrations of Cd, Cu, Fe, and Zn (Table 2) are comparable to those reported for *Pt. capillacea* collected from Abu-Qir Bay (Mohamed and Khaled 2005). The abundance of the macronutrient Ca and the micronutrient Fe in *Pt. capillacea* (Table 2) has been previously published by Wassef et al. (2013), Khairy and El-Sheikh (2015), and Mohy El-Din and El-Ahwany (2016). The tabulated high concentration of Co and Ni in *Pt. capillacea* (Table 2) has also been previously reported by Mohy El-Din and El-Ahwany (2016). The abundance of Ca and Mg in red seaweed collected from Alexandria shorelines has been previously reported by Rashad and El-Chaghaby (2020). The predominance of Ca and K macronutrients, with the sequential abundance of Ca > Mg > P and low concentrations of undesirable As and Hg heavy metals, have been previously reported for *Pterocladia* collected from the Lebanon shoreline (Sebaaly et al. 2012). The Pb concentration 0.001 ± 0.0012 mg/g reported in Table 2 is comparable to that reported by Mohy El-Din and El-Ahwany (2016). The order of the micronutrients in Table 2 (Fe > Zn > Cu) matches what was found in red seaweed collected from the shores of Alexandria (Rashad and El-Chaghaby 2020). According to Álvarez-Viñas et al. (2019), seaweed are characterized by the presence of considerably high concentrations of macronutrients (K, Ca, and Mg), and the most abundant micronutrient is Fe, followed by Zn and Cu. It is worth mentioning that the Pb, As, and Cd concentrations in the collected *Pt. capillacea* biomass (Table 2) are below the maximum permitted amount set by the World Health Organization (WHO) in food and medicinal products, which are 10, 1.0, and 0.3 mg/kg, respectively (Syaharuddin 2019). Furthermore, the concentrations of As, Cd, Pd, and Hg listed in Table 2, are within the international limits established by the European Union, China, Hong Kong, Taiwan, France, and Germany for seaweeds or seaweed-based products intended for human intake and animal fodder, which are ≤ 40, 3, 10, and 0.5 mg/kg, respectively (Guo et al. 2023).

The pH of the *Pt. capillacea* biomass is 7.45 ± 0.05, the total amount of $N + P_2O_5 + K_2O$ is $5.48 \pm 0.07\%$, and the amounts of organic matter and carbon are $27.71 \pm 0.26\%$ and $16.11 \pm 0.15\%$, respectively (Table 3). As shown in Tables 2 and 3, the *Pt. capillacea* biomass has the right amount of minerals and chemicals to meet the Egyptian standard for solid organic fertilizer (8079/2017) and the African organic fertilizer standard ARSO (1490/2018), which would recommend its applicability in organic fertilizer industry (El-Gendy et al. 2023).

The tabulated cellulose content of 19 ± 0.5 (Table 1) is comparable to that reported by Abu Hafsa et al. (2021). Nallasivam et al. (2022) stated that red seaweed still has basic lignin-making processes that are found in land plants. This is probably because they share a common ancestor before they split off into their own evolutionary trees. That might explain the relatively high content of lignin 7 ± 0.5 listed in Table 1. The carbohydrate content of the collected *Pt. capillacea* of approximately $42.16 \pm 0.3\%$ (w/w) (Table 1) is within the recommendable amount for bioethanol production from seaweed, which ranges between 40 and 77% (Offei et al. 2018). Furthermore, the recorded cellulose content (Table 1) falls within the recommended range of 10 to 15% for seaweeds used in biofuel production (Winarni et al. 2022).

Based on the proximate analysis performed, the biomass of *Pt. capillacea* (Table 1) has a calorific value of 16.16 ± 0.5 MJ/kg. It is within the reported values for red seaweed, which ranged between 4.44 and 14.15 MJ/kg (Gamero-Vega et al. 2020). This is comparable to solid

Table 1 *Pterocladia capillacea* biomass analysis

The nutritional makeup							
Dry matter	**Protein**	**Fiber**	**Carbohydrate**	**Lipid**	**Ash**		
wt% (w/w)							
89.11±0.3	6.89±0.31	20.15±0.2	42.16±0.3	2.51±0.05	17.4±0.5		
The proximate analysis							
Moisture	**Volatile**	**Fixed**	**Ash**	**Calorific value**			
wt% (w/w)				**MJ/kg**			
10.89±0.3	69.5±0.5	2.2±0.5	17.4±0.5	16.16±0.5			
The biochemical analysis							
Hemicellulose	**Cellulose**	**Lignin**					
wt% (w/w)							
25±0.5	19±0.5	7±0.5					
Value-added products yields							
Natural pigments mg/g					**Hydrocolloids wt% (w/w)**		**Other biopolymer wt% (w/w)**
Chlorophyll	**Carotenoids**	**Phycocyanin**	**Allophycocyanin**	**phycoerythrin**	**Carrageenan**	**Agar**	**Cellulose**
5.05±0.05	2.12±0.05	1.33±0.05	3.07±0.05	0.97±0.05	28.21±2.5	20.46±1.5	20.15±1.5

Table 2 Mineral composition of the collected *Pterocladia capillacea* biomass

	Macronutrients mg/kg				Micronutrients mg/kg				Undesirable heavy metals mg/kg						
	P	K	Ca	Mg	Fe	Zn	Mn	Cu	Ni	Cd	Cr	Pb	As	Hg	Co
Pt. capillacea	33.71 ± 0.5	301.22 ± 0.5	2471.2 ± 0.5	51.12 ± 0.5	108.19 ± 0.5	40.11 ± 0.5	10.98 ± 0.5	5.01 ± 0.5	0.894 ± 0.05	0.425 ± 0.05	0.481 ± 0.05	0.001 ± 0.0012	0.0011 ± 0.0012	0.00001 ± 0.0	1.02 ± 0.05
Egyptian organic fertilizer standard 8079/2017	–	–	–	–	–	Max 300	–	Max 100	Max 180	Max 5	Max 300	Max 300	–	Max 4	Max 100
African organic fertilizer standard ARSO (1490/2018)			Max 1%	Max 0.5%	1000–2500	40–1000	200–800	8–300	Max 50	Max 5	Max 50	Max 30	Max 10	Max 2	0.5–1
Solid biofuels ISO 17225–1	–	–	–	–	–	≤ 100	–	≤ 20	≤ 10	≤ 0.5	≤ 50	≤ 10	≤ 1	–	– – –

biofuel derived from lignocellulosic material (Al-Sadek et al. 2021). It is also comparable with those reported for the green *Ulva fasciata* and brown *Sargassum latifolium*, which recorded 15.19 MJ/kg (El-Gendy et al. 2023) and 14.82 MJ/kg (El-Gendy et al. 2024), respectively and recommended to be used as solid biofuel discs. Moreover, both the tabulated contents of detrimental ash and heavy metals (Tables 1 and 2) are low and within the acceptable ranks set by the International Organization for Standardization (ISO 17225–1, 2014) for solid biofuels.

A sequential extraction process for valorization of *Pterocladia capillace* biomass into numerous valued compounds

Natural pigments

The actone:methanol extraction yielded approximately 2.95 ± 0.5 (wt% w/w) natural pigments. Figure 3 shows the UV/Vis spectrum of *Pt. capillacea* extract. It shows that carotenoids, chlorophyll (a), and the red coloring pigments phycoerythrin and phycocyanin are the main components. That recorded 3.49 ± 0.05 mg/g chlorophyll(a), 1.18 ± 0.05 mg/g *β*-carotene, 1.33 ± 0.05 mg/g phycocyanin, 3.07 ± 0.05 mg/g allophycocyanin, 0.97 ± 0.05 mg/g phycoerythrin, 5.05 ± 0.05 mg/g total chlorophyll, and 2.12 ± 0.05 mg/g carotenoids (Table 1). The carotenoids/chlorophyll (a) ratio recorded approximately 0.607 ± 0.05. It is slightly higher than that recorded for *Pt. capillacea* collected by Ismail and Osman (2016), which ranged between 0.426 and 0.459 within summer and autumn, respectively. The red seaweed is known for the predominance of chlorophyll (a) over the chlorophyll (b), where the carotenoids and chlorophyll (a) usually range between 0.2–1.8 and 0.35–9.8 mg/g, respectively (Álvarez-Viñas et al. 2019). Lutein and *β*-carotene are reported in red seaweed (Álvarez-Viñas et al. 2019; Cherry et al. 2019; Freitas et al. 2022; Carpena et al. 2023). Álvarez-Viñas et al. (2019) reported that generally, the phycocyanin and phycoerythrin contents in red sewed can range between 0.02–10 and 0.8–7 mg/g, respectively.

The concentrations of phycobiliproteins (phycoerythrins, phycocyanin, and allophycocyanin) recorded in this study are comparable to those reported by Ismail and Osman (2016). Phycobiliproteins can range between less than 1 mg/g up to as high as 125 mg/g in red seaweed (Álvarez-Viñas et al. 2019). According to Haryatfrehni et al. (2015), Rhodophyta red seaweed are the main sources of the valuable water-soluble, light-harvesting protein and antioxidant phycoerythrin. El-Sayed and Ismail (2022) reported that the red color of red seaweed distinguishes it due to the predominance of phycoerythrin and

Table 3 The physicochemical inspection of the collected *Pterocladia capillacea* biomass in comparison with the Egyptian organic fertilizer standard

Parameter	*Pt. capillacea*	Egyptian organic fertilizer standard (8079/2017)	African organic fertilizer standard ARSO (1490/2018)
Electrical conductivity dS/m	10.33 ± 0.03	6–10	Max 5
Total dissolve solids (mg/L)	6611.2 ± 19.2	3840–6400	–
Organic C %	16.11 ± 0.15	Min 15	Min 12
Organic matter %	27.71 ± 0.26	Min 18	Min 7
Moisture content %	9.91 ± 0.3	Max 70	10–35
Total nitrogen %	1.10 ± 0.05	Min 0.28	Min 1
P_2O_5%	0.77 ± 0.01	Min 0.8	–
K_2O %	3.61 ± 0.01	Min 0.8	–
$N + P_2O_5 + K_2O$ %	5.48 ± 0.07	Min 4	Min 5
C/N	14.65 ± 0.2	18–22:1	≤ 20:1
pH	7.45 ± 0.05	6–8	6.6–7.5

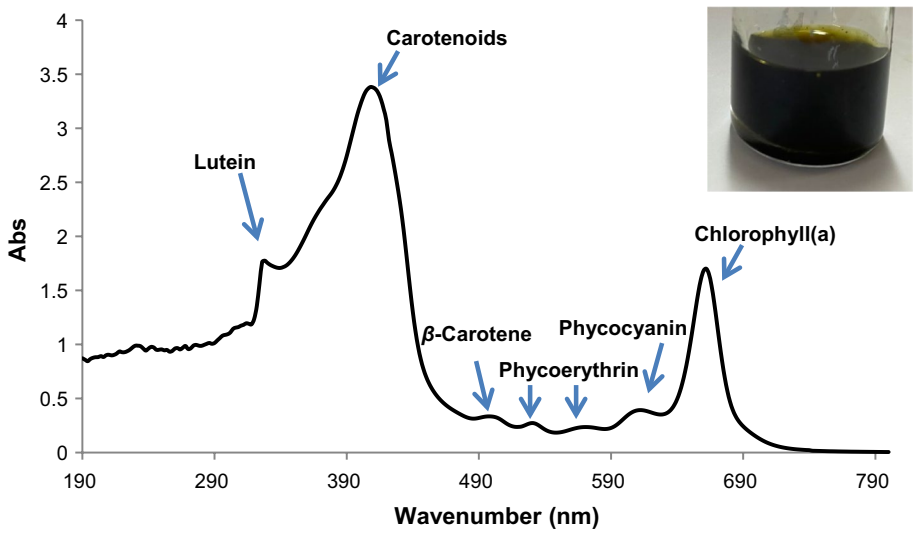

Fig. 3 UV/Vis spectra of acetone:methanol (1:1) extract of *Pterocladia capillacea*

phycocyanin. The mineral and β-carotene contents differ in seaweed according to seasons, acquaintance with waves, geographical dispersion, physiological changes, and environmental conditions (Khairy and El-Sheikh 2015). However, the abundance of β-carotene in *Pt. capillacea* has been previously published by Khairy and El-Sheikh (2015). *Pt. capillacea* has been reported to contain chlorophyll as well as phycoerythrin, an accessory photosynthetic pigment (Al-Saeedi et al. 2023). Freitas et al. (2022) reported that Rhodophyta red seaweed is valuable source of phycobiliproteins (i.e., phycoerythrins, phycocyanin, and allophycocyanin), carotenes (i.e., carotenoids and xanthophylls), and chlorophyll a.

Carrageenan

The collected *Pt. capillacea* yielded approximately 28.21 ± 2.5% (w/w) carrageenan (Table 1). That is roughly twice the amount extracted from *Pterocladia* collected from the Lebanon seashore (Sebaaly et al. 2012). The carrageenan yield is reported to differ with environmental conditions, red seaweed species, harvesting season, and extraction procedure (Al-Nahdi et al. 2019). However, studies have reported a range of 22 to 71% in red seaweed (Øverland et al. 2019).

The bimodal particles size distribution of carrageenan (Fig. 4a) reveals the predominance of 413 nm particles over the 0.53 µm ones, with a total average particles size of 773.9 nm, a polydispersity index (PDI) value of 0.611, and a zeta potential of − 28.8 mV. The FESEM (Fig. 4d) confirms the existence of aggregates, as suggested by the DLS analysis.

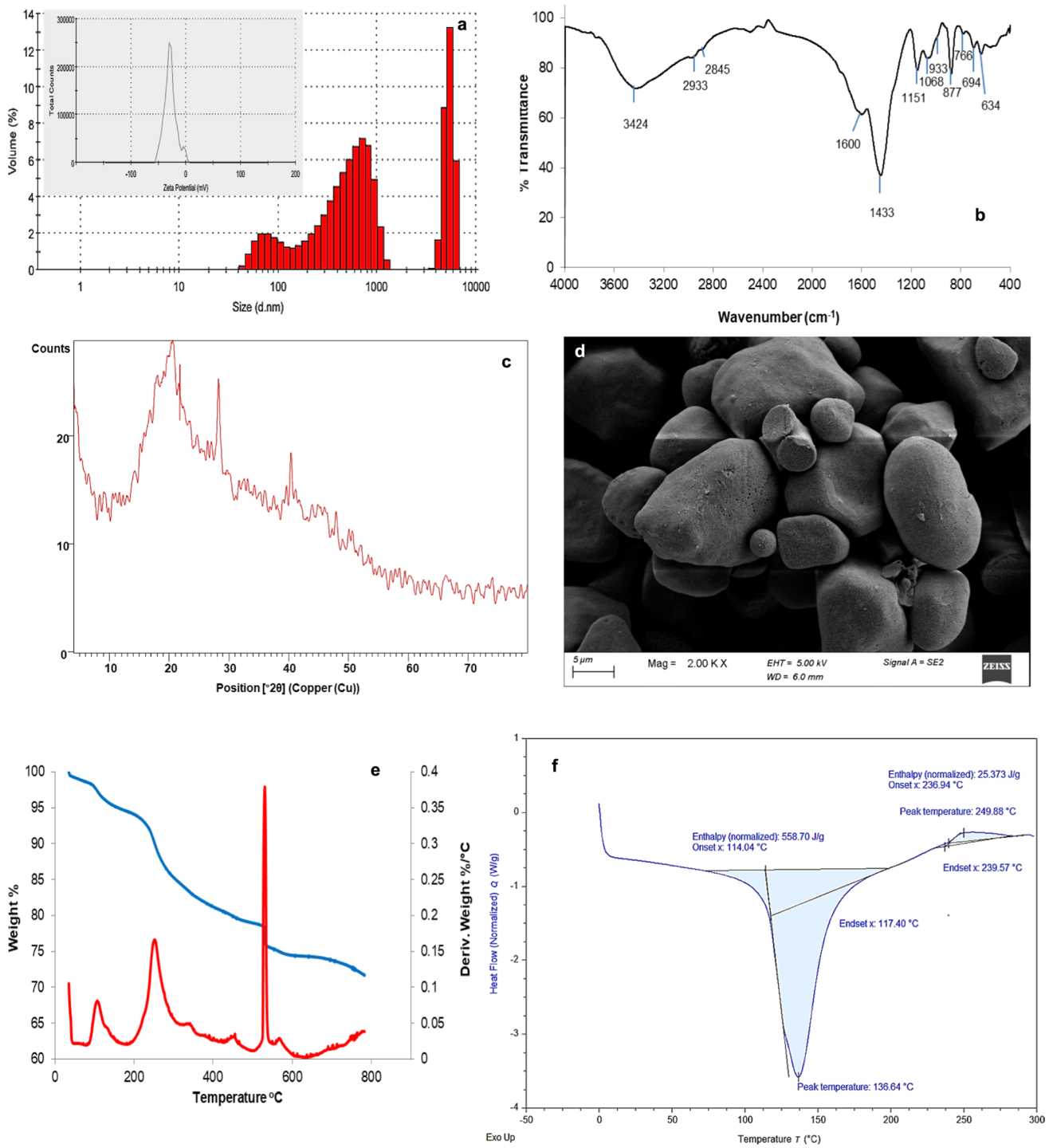

Fig. 4 The DLS and zeta potential (**a**), FTIR (**b**), XRD (**c**), FESEM (**d**), TGA (**e**), and DSC (**f**) of the extracted carrageenan

Figure 4b shows an FTIR spectrum that matches the one shown by Ismail and Amer (2020) for carrageenan taken from the red seaweed *Pt. capillacea* and *Corallina officinalis*. It is possible, according to Sebaaly et al. (2012), to interpret the broad peak located at 3424 cm^{-1} as the result of O–H stretching vibration. The small peaks at 2933 and 2845 cm^{-1} can be attributed to the C–H, O–CH_3 stretching vibrations, respectively (Ismail and Amer 2020). The peaks around 1600 and 1433 cm^{-1} can be attributed to the uronic acid C = O groups' symmetric and asymmetric vibrations. The sulfate groups' S = O and C–O–S stretching is indicated by the FTIR bands at 1151 and 877 cm^{-1}, respectively. The

characteristic peaks of red seaweed' agarocolloids appear around 766 cm^{-1} (Ismail and Amer 2020). The band at 1068 cm^{-1} corresponds to the galactan skeleton of ƙ–carrageenan (Al-Nahdi et al. 2019). The band at 933 cm^{-1} in the spectra can be attributed to 3,6–anhydrogalactose bridge, which is prevalent in ι–and ƙ–carrageenan but not in λ–carrageenan (Wahlström et al. 2018). The absence of peaks at 1214 and 805 cm^{-1} would indicate that the extracted carrageenan does not match with the ι–carrageenan (Abdul Ghani et al. 2019) and matched more with ƙ–carrageenan (Han et al. 2021; Rudke et al. 2024).

The XRD pattern (Fig. 4c) depicts the wide characteristic peak of carrageenan around 2θ (22°) and another less shoulder hump around 2θ (32°). That coincides with the semi-crystalline ƙ–carrageenan polysaccharide with an elevated amorphous nature (Kulal and Badalamoole 2020; Perumal and Selvin 2020; Li et al. 2024). The other sharp peaks around 2θ (29° and 42°) appeared in the XRD pattern (Fig. 4c) might be according to Serra et al. (2023) attributed to the presence of impurities. The FESEM micrograph (Fig. 4d) reveals amorphous and irregular-shaped micro-sized granules. Dewi et al. (2015) reported a similar observation for *Kappaphycus alvarezii* carrageenan.

The TGA thermograph (Fig. 4e) is well matched to that illustrated for carrageenan extracted from the red seaweed *Porphyra umbilicalis* Kützing (Wahlström et al. 2018). The first degradation phase with weight loss of approximately 1.42% occurred between 35 and 100 °C, and may be ascribed to the moisture loss. The second sharp degradation phase occurred with an approximate weight loss of 20.28% between 180 and 450 °C, which peaked at approximately 247 °C and may be related to the disintegration of the carbohydrate backbone and emission of sulfur dioxide (Jumaah et al. 2015). The third degradation phase of the decomposition of the carrageenan's network structure occurred between 470 and 600 °C, proceeded slowly, peaked at approximately 530 °C, and represented a weight loss of approximately 25.57%. The recorded low total weight loss of approximately 25.57% would according to Kulal and Badalamoole (2020), indicate the thermal stability of the extracted ƙ–carrageenan. The DSC thermograph (Fig. 4f) with the exothermic peak at 239.57 °C, representing the carrageenan degradation, matches well that reported by Elnashar and Yassin (2009) for pure ƙ–carrageenan.

The antimicrobial activity of the extracted carrageenan Table 4 tabulates the antimicrobial activity of the extracted *Pt. capillacea* carrageenan against various pathogenic microorganisms, besides its activity index relative to standard microbial agents. It is found to express an efficient antimicrobial activity against a wide array of different pathogenic microorganisms with a high statistically significant difference between the computed activity indices ($p < 0.0001$). The antimicrobial activity of carrageenan is reported to differ with the algal species extracted from and the pathogenic microorganisms (Ismail and Amer 2020). In this study, the extracted carrageenan was more effective against yeast strains than bacteria (Table 4), with a statistically higher activity index ($p < 0.0001$). Wang et al. (2012) reported a similar observation. Moreover, the relatively high antifungal and antibacterial activities of carrageenan against *A. niger* and the Gram + ve *B. subtilis* and *S. aureus* have been previously reported by Ismail and Amer (2020). The extracted carrageenan expressed a statistically higher biocide activity against fungi relative to the other studied pathogenic microorganisms ($p < 0.0001$). The superiority of carrageenan as an antifungal agent has also been reported by Soares et al. (2016) and attributed that to the possible occurrence of alterations in chitin and β-glucan fungal cell wall contents. The efficient antimicrobial activity of k-carrageenan polyanions against the Gram + ve *S. aureus* and *C. albican* has been previously reported by Souza et al. (2018). That was attributed to the decrease of chitin and β-glucan in *C. albican* cell wall. Moreover, the Gram + ve bacteria are known to have a high content of mucopeptide and peptidoglycan lipids, which would enhance the electrostatic interaction with the negatively charged sulfate groups in carrageenan (Javadiyan et al. 2022). Also, glycoprotein receptors on the surface of the carrageenan would recognize and bind to charged compounds on the bacterial cell surface, cytoplasmic membrane, and DNA. This would increase the permeability of the cytoplasmic membrane, cause cells to break down, proteins to leak out, and DNA structure to become less stable, which would slow down transcription and translation (Ismail and Amer 2020). The low antibacterial effect against the Gram –ve *E. coli* with a high statistical difference relative to the other studied pathogenic microorganisms ($p < 0.0001$) might be related to the occurrence of repulsion between the negatively charged sul-

Table 4 The antimicrobial activity of the extracted carrageenan and activity index relative to standard antibiotic

Tested microorganism Compound ID	*B. subtilis* ATCC 6633	*S. aureus* ATCC 35556	*E. coli* ATCC 23282	*P. putida* ATCC 10145	*C. albicans* IMRU 3669	*A. niger* ATCC 16404
Carrageenan	27 ± 0.51	28 ± 0.60	14 ± 0.30	29 ± 0.50	30 ± 0.55	35 ± 0.80
Reference antibiotic	35 ± 0.7	35 ± 0.7	22 ± 0.44	33 ± 0.66	26 ± 0.52	22 ± 0.44
Activity index	0.77 ± 0.08	0.8 ± 0.01	0.64 ± 0.02	0.88 ± 0.01	1.15 ± 0.01	1.59 ± 0.01

fate groups in the carrageenan molecule and the negatively charged bacterial cell wall (Amorim et al. 2012). It might also be attributed to the extra shelter given by the high content of phospholipids and lipopolysaccharides in the outer cell membrane (Jasem et al. 2023). Moreover, Pradhan and Ki (2023) reported the antimicrobial activity of the carrageenan molecule might be attributed to its binding to the DNA limiting, its transcription and translation.

Agar

The collected *Pt. capillacea* yielded approximately 20.46 ± 1.5% (w/w) agar (Table 1). That matches well with agar yields extracted from *Pt. capillacea* that was collected from the Egyptian Alexandria beach (Rao and Bekheet 1976). It is also comparable to yielded agar from *Pt. capillacea* collected from Abu-Qir Bay during August and September (Fathy and Mohammady 2007). It is within the range reported for Spanish *Pt. capillacea*, which yielded from 15 to 29.8% agar depending on the harvesting season (Freile-Pelegrín et al. 1996). The obtained agar yield in this study aligns with the reported range for Syrian *Pt. capillacea*, which ranges from 11% to 35.46% agar based on the applied extraction time (Mayhoob et al. 2017). Agar yield from worldwide *Pt. capillacea* varies between 5 and 34%, depending on the geographical distribution, ecological and environmental conditions, algal species, growth and harvesting seasons, and extraction techniques (Patarra et al. 2020).

The DLS analysis (Fig. 5a) indicates agar with an average granular size of about 601.6 nm, a PDI value of 0.261, and a zeta potential of − 34.2 mV.

The FTIR spectrum (Fig. 5b) matches well with that of agar extracted from the red seaweed *Gracilaria tikvahiae* (Rocha et al. 2019) and *Gracilaria* species (Vuai 2022). The peaks at 3392 cm^{-1} and 3288 cm^{-1} are related to the O–H and N–H stretching (Ibrahim et al. 2015). The peaks around 2940 cm^{-1} and 2874 cm^{-1} correspond to the C–H, O–CH_3 stretching vibrations, respectively (Xiao et al. 2021). The most distinctive bands were found in the 850–1456 cm^{-1} range, which is according to Belattmania et al. (2021) commonly identified as agarocolloid. The peak at 1382 cm^{-1} can be assigned to the ester sulfate (Aguiar et al. 2023). The small peaks appear between 1274 and 1224 cm^{-1} are attributed to the sulfate groups of α-L-galactose 6-sulfate. The peaks appear between 1124 and 1112 cm^{-1} are associated to the agar galactan skeleton (Xiao et al. 2021). The characteristic agar bands of 3,6-anhydro-galactose bridges appear at 1068 and 929 cm^{-1} (Rocha et al. 2019). The band at 1633 cm^{-1} can be attributed to the stretching of the conjugated peptide bond formed by NH and C = O groups (Ibrahim et al. 2015), while the peak at 600 cm^{-1} is related to the N–H out of plan vibration (Chaudhary et al. 2020). That might indicate the presence of protein and/or incomplete removal of pigments (Xiao et al. 2021). The peak that appears at 850 cm^{-1} might be attributed to the presence of sulfate groups (Rocha et al. 2019). The galactose ring's skeleton bending is responsible for the peaks at 760 and 787 cm^{-1} (Rocha et al. 2019; Vuai 2022).

The XRD pattern of the extracted agar (Fig. 5c) depicts a diffused wide peak around 2θ (20°), a shoulder at 2θ (13.9°), and another smaller wide peak at 2θ (19°). This could potentially represent an amorphous agar with a somewhat ordered structure, as suggested by Martínez-Sanz et al. (2019). That organized structure could be because of the double-helical shape made by the intermolecular hydrogen bonding (Zhang et al. 2019). The FESEM micrograph (Fig. 5d) reveals amorphous spherical and cuboidal-shaped micro-sized granules.

The TGA of the extracted agar (Fig. 5e) matches well with that of the agar extracted from the red seaweed *Gracilaria tikvahiae* (Rocha et al. 2019). The thermograph depicts two main regions of weight loss. The first occurs around 100 °C, with a weight loss of approximately 14.39% and may be attributed to the moisture loss. The main weight loss starts from approximately 190 °C and peaked at approximately 285 °C. Martínez-Sanz et al. (2019) reported a similar observation for *Gelidium sesquipedale* agar, which is according to Ding et al. (2020) attributed to the carbohydrate decomposition. The observed continual weight loss until the occurrence of almost complete decomposition within 650 °C (Fig. 5e) has also been reported by Oprea (2010) and Maleki et al. (2019). The endothermic peaks that appeared at 164.18 °C and 225.25 °C in the agar DSC graph (Fig. 5f) might be, according to Pino-Ramos et al. (2021), attributed to the agaropectin and agarose decomposition, respectively.

Cellulose

The collected *Pt. capillacea* yielded approximately 20.15 ± 1.5% (w/w) cellulose (Table 1). Researchers report that the cellulose content in red seaweed ranges from 0.9 to 8.7% (w/w), with *Pterocladia heteroplatos* having the highest recorded content (Siddhanta et al. 2013). However, Siller-Sánchez et al. (2019) reported that the cellulose content in red seaweed ranges from 13 to 19% (w/w), whereas Baghel et al. (2021) reported a range of 0.85 to 18% (w/w). However, Doh et al. (2020) reported that the cellulosic nanocrystals in red seaweed range from 13.3 to 17.4% (w/w).

The DLS analysis proves the bimodal particles size distribution of the extracted *Pt. capillacea* cellulose (Fig. 6a), which indicates the presence of some aggregates. It also shows that 89.53 nm particles are more common than 787.1 nm particles. The average particle size is 90 nm, the PDI value is 0.509, and the zeta potential is − 30.5 mV. According to Naduparambath et al. (2018), a stable suspension of nano-crystalline cellulose occurs when its zeta potential falls below -30 mV or rises above + 30 mV.

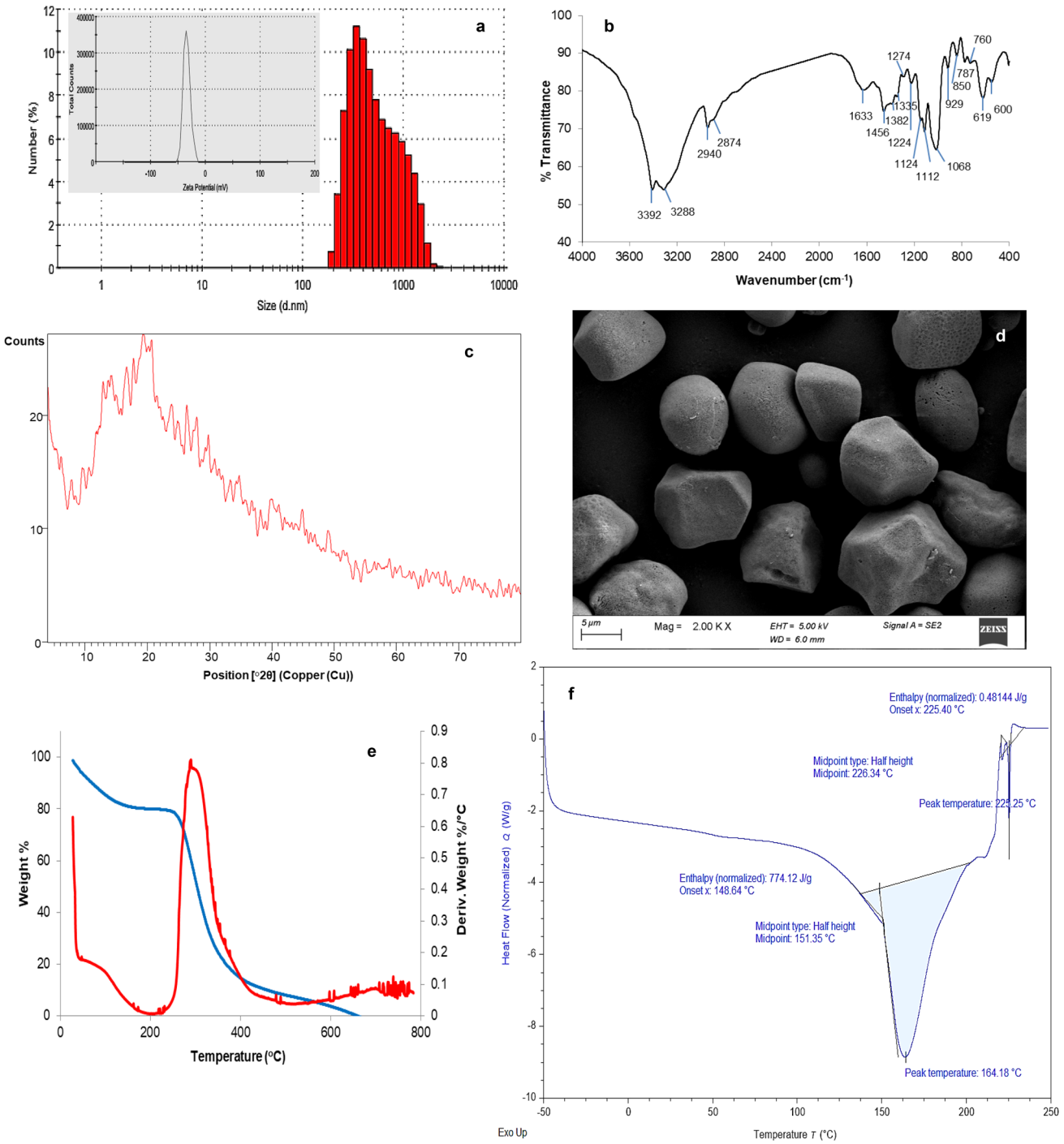

Fig. 5 The DLS and zeta potential (**a**), FTIR (**b**), XRD (**c**), FESEM (**d**), TGA (**e**), and DSC (**f**) of the extracted agar

The broad peak at 3414 cm^{-1} and the sharp peak at 1647 cm^{-1} in the FTIR spectrum (Fig. 6b) are related to the O–H stretching and bending vibrations, respectively of cellulose (Doh et al. 2020). The peaks at 2914 and 1440 cm^{-1} are attributed to the cellulosic $–CH_2$ symmetric and asymmetric stretching vibration, respectively (Wahlström et al. 2020; El-Gendy et al. 2023; 2024). The peak at 1062 cm^{-1} is attributed to the CH_2–O–CH_2 stretching vibrations of the pyranose ring. The cellulosic polysaccharides can be confirmed by the existence of the distinguishing weak FTIR-vibrational band of the β-glycosidic bond at 899 cm^{-1} (Muthukumar and Chidambaram 2022). The broadening of the major peak at 3414 cm^{-1} is gesturing the occurrence of numerous numbers of hydrogen bonding (El Achaby et al.

2018b, a; Varma et al. 2022). The lack of vibrational bands in the range of 1700–1740 cm^{-1} (Fig. 6b), which correspond to the acetyl or uronic ester groups, would indicate the purity of cellulose from hemicellulose (Jmel et al. 2016). Moreover, the absence of peaks of the sulfate groups at 1112–1151, 1274–1224, and 850–877 cm^{-1} and the characteristic peaks of red seaweed' agarocolloids at 766 and 930 cm^{-1}, would assure the purity of cellulose from carrageenan and agar. However, the presence of the two weak peaks at 1440 and 1550 cm^{-1} would be attributed to the aromatic ring's C = C of lignin (Lakshmi et al. 2017; El Achaby et al. 2018b, a).

The XRD pattern of the extracted *Pt. capillacea* cellulose (Fig. 6c) aligns with that of cellulose I (card number 00–056-1717), which has a chemical formula of $(C_6H_{10}O_5)$. According to Siddhanta et al. (2009), cellulose I is recognized as the natural and dominant crystalline structure

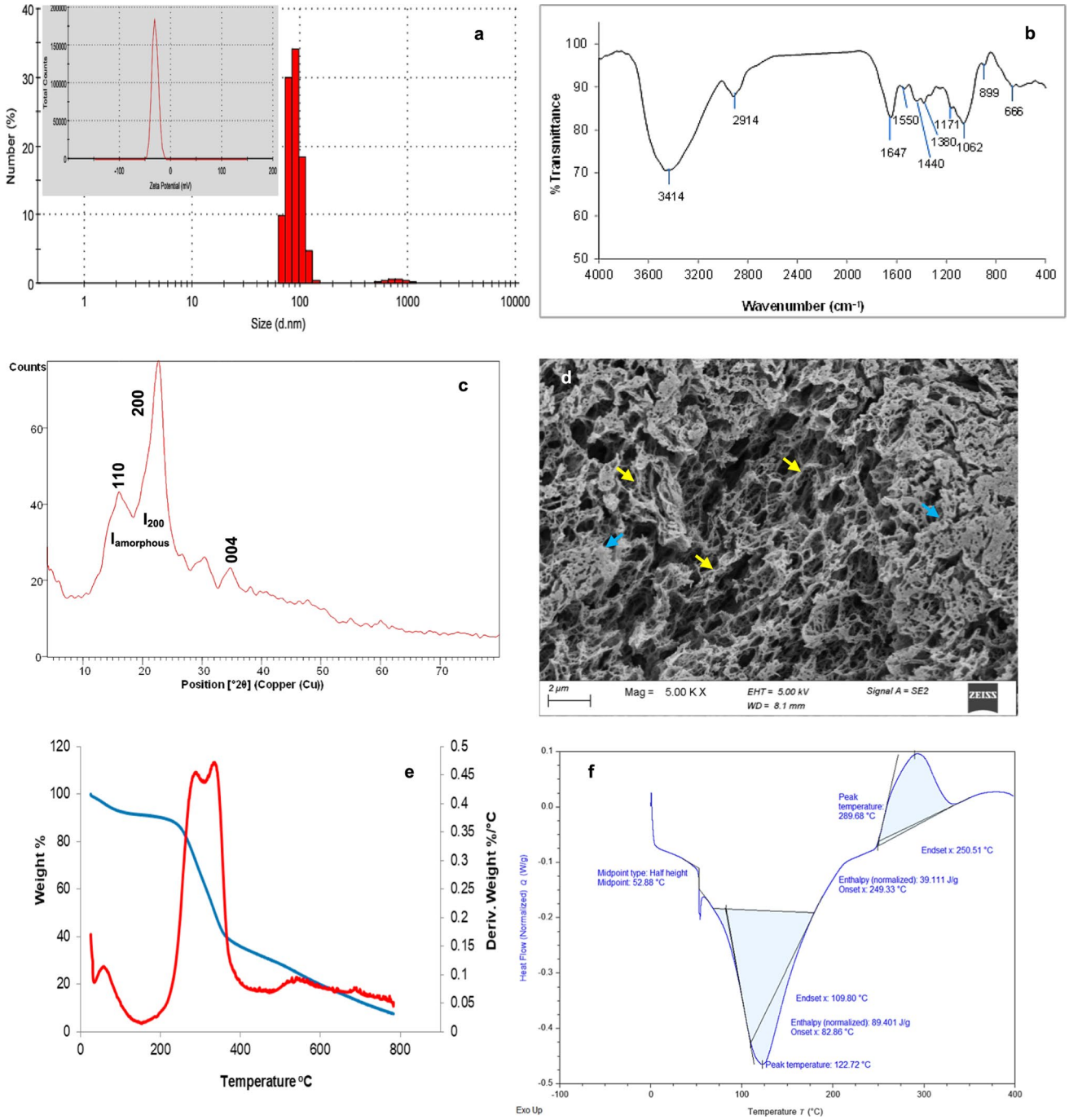

Fig. 6 The DLS and zeta potential (**a**), FTIR (**b**), XRD (**c**), FESEM (**d**), TGA (**e**), and DSC (**f**) of the extracted cellulose

of cellulose found in seaweed. The 200-plane diffraction, which is an indicator of the cellulose crystallinity, appears at 22.72° (Fig. 6c). The broadness of peak at (2θ) 16.07° (Fig. 6c) might indicate the merging of the crystallographic planes $\bar{1}10$ and 110 and is known to refer to the amorphous phase. A similar observation has been published for cellulose extracted from agar-industry red seaweed residues (López-Simeon et al. 2012). The peak at 34.87° (Fig. 6c) corresponds to the crystallographic plane 004. The XRD pattern matches well with the crystalline cellulose extracted from the red seaweed *Gelidium elegance* (Lee et al. 2008) and the micro-crystalline cellulose extracted from the red seaweed *Eucheuma cottonii* (Han et al. 2022), *Gracilaria verucosa*, and *Eucheuma cottonii* (Nissa et al. 2023).

The crystallinity index (CrI%) was computed in accordance with Doh et al. (2020).

$$CrI\% = \left(\frac{I_{200} - I_{amorphous}}{I_{200}}\right) \times 100 \quad (9)$$

where I_{200} is the peak intensity of diffraction from the 200 lattice plane at (2θ) 22.72°, and $I_{amrophous}$ is the trough intensity assigned to the amorphous section at (2θ) 16.07° (Fig. 6c). This analysis revealed that the extracted crystalline cellulose had a CrI% of approximately 78.60%. It is comparable to that of microcrystalline cellulose reported by Han et al. (2022). The elevated occurrence of inter- and intra-molecular H-bonding and the cellulosic-fibril structure could potentially explain the elevated CrI% (Bhutiya et al. 2020; Doh et al. 2020). The crystallinity index of cellulose extracted from seaweeds and other natural sources is commonly expected to range between 41.4 and 71.5% (Hai et al. 2015; Doh et al. 2020).

The FESEM micrograph (Fig. 6d) reveals cellulosic nanofibers. The micrograph demonstrates a layered and densely cross-linked web-like structure (blue arrows, Fig. 6d) composed of numerous filaments, or fibrous helixes (yellow arrows, Fig. 6d). Similar observation has been reported for cellulose extracted from the red seaweed *Porphyra umbilicalis* Kützing (Wahlström et al. 2018), *Eucheuma cottonii* and *Gracilaria verucosa* (Nissa et al. 2023), and some other edible seaweed (Muthukumar and Chidambaram 2023).

The TGA/DTG thermograph (Fig. 6e) reveals a first weight loss occurrence between 25 and 125 °C, representing the moisture loss. The main decomposition occurred within the temperature range of 200 to 400 °C, with split peaks at 280 and 350 °C. Cellulosic glycosidic linkages, hydroxyl and methyl hydroxyl groups, and possible propanoid side chain degradation are responsible for the main decomposition region (Dorez et al. 2014; Bhutiya et al. 2020; Varma et al. 2022). However, the small shouldered peaks at 527 and 675 °C would indicate the presence of traces of lignin, as these peaks are related to the condensation and rearrangements of lignin-aromatic construction (Dorez et al. 2014). That confirms the FTIR interpretation (Fig. 6b). The DSC thermograph (Fig. 6f) shows an exothermic peak with a peak temperature T_p at 289.68 °C and enthalpy ΔH of 39.11 J/g, proving the thermal stability of the extracted cellulose (El-Gendy et al. 2023). That is the same temperature that was previously reported for red seaweed cellulose to break down (Hai et al. 2015), which was because it had a high crystallinity index. The main endothermic peak at T_p122.72 °C with an enthalpy change ΔH 89.40 J/g (Fig. 6f) would be, according to Cichosz and Masek (2019), due to the evaporation of trapped water and the breakage of hydrogen bonding in the cellulosic construction.

The acquired valued products and their proposed potential uses

In 2019, the global seaweed market was valued at US$ 11.8 billion and is projected to attain US$ 22.13 billion by 2024, reflecting an annual growth rate of around 8.9% (Sultana et al. 2023). Red seaweed constitutes 61% of global seaweed production (Álvarez-Viñas et al. 2019), and it is anticipated to rise due to the economic significance of its hydrocolloid food ingredients, namely carrageenan and agar (Pessarrodona et al. 2024). This study promotes the promising market potentially of red seaweed *Pt. capillacea*. The nutritional and mineral composition of the collected *Pt. capillacea* (Table 1 and 2) recommends its safe practice in the food, pharmaceutical, and animal fodder industries. The *Pt. capillacea* elevated concentrations of Ca, Fe, and K (Table 2), would suggest its application as a food supplement. According to Sebaaly et al. (2012), when used as a food supplement, *Pterocladia*'s elevated concentrations of Ca and K can aid in bone formation and reduce high blood pressure. It can also aid in overcoming the human Fe deficiency, provided that the daily allowance for Fe intake is limited to 10 mg (Sebaaly et al. 2012). In addition, its Zn content (Table 2) is beneficial because it is an essential cofactor for certain enzymes (Sebaaly et al. 2012). *Pt. capillacea* has been reported as an efficient supplement to enrich balady bread organoleptic characteristics (Yousef et al. 2015). Øverland et al. (2019) reported the possibility of using dried and milled red seaweed as animal feed. The European seabass (*Dicentrarchus labrax*) fry has been reported to benefit nutritionally from the addition of *Pt. capillacea* to their formulated meals (Wassef et al. 2013). *Pt. capillacea* has been reported as nutritive supplements for Nile tilapia fingerlings (Khalafalla and El-Hais 2015) and rabbits (Abu Hafsa et al. 2021).

The collected *Pt. capillacea* in this study may provide humans with beneficial components such as protein, fat,

carbohydrates, and carotenoids. Mohy El-Din and El-Ahwany (2016) reported that pigments such as carotenoids and chlorophylls may be the source of the marine seaweed's antioxidant activity. Furthermore, the phycoerythrin that *Pt. capillacea* contains is beneficial; according to Ismail and Osman (2016), phycoerythrin is the most commonly used phycobiliprotein in immunology, cell biology, cosmetics, food, fluorescent probes, and pharmaceutical applications. According to Khairy and El-Sheikh (2015), antioxidants, particularly carotenoids, help to counteract the damage free radicals cause, which is associated with aging. It has been reported that natural β-carotene is ten times easier for the body to absorb than synthetic β-carotene. Consequently, eating a diet high in carotenoids, especially β-carotene, can decrease the chance of developing cancer (Khairy and El-Sheikh 2015).

It is also advised to use the collected *Pt. capillacea* as an environmentally friendly organic fertilizer, minimizing the agricultural chemical footprint due to its specified mineral composition (Table 2) and chemical contents (Table 3), which match well with the Egyptian organic fertilizer standards (El-Gendy et al. 2023; 2024). The aqueous extract of *Pt. capillacea* has been reported to enhance the growth and yield, besides the minerals, chlorophyll a,b, and antioxidants constituents of Jew's Mallow (Ashour et al. 2020).

The relatively high carbohydrate and holocellulose (cellulose and hemicellulose) contents listed in Table 1, recommend the applicability of *Pt. capillacea* in liquid biofuels (biobutanol and bioethanol) production (Soliman et al. 2018; del Río et al., 2020; Osman et al. 2020; El-Gendy et al. 2024). Moreover, the calorific value of the dried biomass of *Pt. capillacea* with its relatively low ash and heavy metals contents (Table 1 and 2) recommend its usage as a primary solid biofuel (El-Gendy et al. 2023; 2024).

The hydrocolloid carrageenan is considered a sulfated galactan and reported to have a wide application in the food industry as a water-holding, gelling, and thickening agent (Ismail and Amer 2020). According to Siller-Sánchez et al. (2019), the food industry uses 70 to 80% of the globally produced seaweed carrageenan, with the remainder finding its way into pharmaceuticals, textiles, and cosmetics. Beaumont et al. (2021) have reported numerous biomedical uses for carrageenan hydrogels. The most common reasons for persistent wound contamination are *P. aeruginosa* and *S. aureus* (Ulagesan et al. 2023). *S. aureus* is a widespread infection that spreads through consumption of polluted food or drink (Pierre et al. 2011). The recorded antimicrobial activity of *Pt. capillacea* carrageenan (Table 4) would recommend its applicability in water densification from pathogenic microorganisms, in addition to the manufacturing of food packaging materials and wound dressing.

The hydrocolloid agar is a lined galactan polysaccharide made up of lengthy agaropectin and agraose chains. It is more commercially valuable than carrageenan (Álvarez-Viñas et al. 2019). It has wide applications in human and animal food, as well as several medical, pharmaceutical, cosmetics, biological, and industrial uses for its exceptional gelling and thickening (Patarra et al. 2020). It has been reported that the quality of *Pterocladia* agar collected from the Egyptian Mediterranean coast is worldwide superior to other red seaweed's extracted agar (Rao and Bekheet 1976; Ibrahim et al. 2015).

Cellulose is a water-insoluble polysaccharide with wide applications in the food, paper, animal feed, textiles, pharmaceutical, healthcare, biodegradable plastics, and biofuel industries (Siddhanta et al. 2013; Doh et al. 2020; Machado et al. 2024). The nano-cellulosic fibril structure of the extracted *Pt. capillacea* cellulose (Fig. 6d) is considered advantageous as it would have wide industrial applications where increased surface area is required (Muthukumar and Chidambaram 2023). The computed crystallinity index of the extracted cellulose enhances its applicability as a reinforcing agent in composites (El Achaby et al. 2018b, a; Nissa et al. 2023). The observed thermal stability of the extracted *Pt. capillacea* cellulose would also promote its applicability in biocomposites and packaging (El-Gendy et al. 2023; 2024). It is worth mentioning that the cellulose yield after the sequential extraction of pigments and hydrocolloids (carrageenan and agar) in this study is exceeding the estimated average cellulose content (6.31%) in the seaweed waste biomass disposed of worldwide phycocolloid manufacturing (Baghel et al. 2021). It also falls within the reported recommended range for seaweed biofuel production, which is between 10 and 15% (Winarni et al. 2022).

Veeragurunathan et al. (2019) reported that the retail price of agar was approximately 18 US$/kg, compared to 10.4 and 12 US$/kg for carrageenan and alginate, respectively. Johnston et al. (2023) reported that the global merchandized prices for agar and carrageenan were 18 and 10.5 US$/kg, respectively. Rudke et al. (2024) report that the price of red seaweed carrageenan; ranges from 5.50 to 9.00 US$/kg, contingent on its purity. Baghel et al. (2021) reported that the current worldwide nano-cellulose market is anticipated to be worth US$ 297 million and will rise to US$ 783 million by 2025, with a compound yearly development rate of 21.3%. Moreover, by the year 2018, the assessed worldwide micro-cellulose market was US$ 885.1 million, which reached US$ 1,241.4 million by the year 2023, with a compound yearly development rate of 7% (Baghel et al. 2021).

Conclusion

This work proposes an eco-friendly and simple sequential fully integrated scheme for generating a variety of valuable bioproducts with varied conceivable commercial

applications from the abundant, immensely flourished, and easily harvestable Mediterranean red seaweed *Pterocladia capillacea*. That bioprocess valorizes the whole *Pt. capillacea* biomass into 3.49 ± 0.05 mg/g chlorophyll(a), 1.18 ± 0.05 mg/g β-carotene, 5.05 ± 0.05 mg/g total chlorophyll, 2.12 ± 0.05 mg/g carotenoids, phycobiliproteins of approximately 1.33 ± 0.05 mg/g phycocyanin, 3.07 ± 0.05 mg/g allophycocyanin, and 0.97 ± 0.05 mg/g phycoerythrin, hydrocolloids of approximately 28.21 ± 2.5% carrageenan and 20.46 ± 1.5% agar, and finally cellulose of approximately 20.15 ± 1.5%.

The Egyptian Mediterranean coastline, *Pt. capillacea* applied in this study, also proved to be an excellent source of lipids, proteins, fibers, and inorganic minerals, as well as carbohydrates. This study also suggests that *Pt. capillacea* biomass is a viable feedstock for the production of various biopolymers, biocide, organic fertilizer, animal feed, and solid and liquid biofuels.

This approach is highly strategic and deliberate, as it does not require fresh water, land, pesticides, or fertilizer; it only requires carbon dioxide, sunlight, and seawater for growth. Therefore, it will reduce carbon and water footprints while also avoiding competition with food crops on agricultural lands, thereby mitigating the negative aspects of the green economy. Additionally, it will open up new markets and enhance the application of green chemistry with its twelve main principles.

In conclusion, the proposed zero-waste biomass residue process has the potential to enhance resource efficiency by converting as much biomass as possible, curb the proliferation of offensive algal biomass along Egypt's Mediterranean Sea coastline, and alleviate the detrimental impacts of harmful algal blooms on tourism, ecosystems, and economic growth. The commonly available red seaweed found throughout the Egyptian Mediterranean Sea shorelines, *Pterocladia capillacea*, instead of being a wasted biomass, can act as a wealthy resource for energy, food, animal fodder, medical, pharmaceutical, cosmetics, textiles, paper, and many other industrial sectors. That would open huge applications of *Pt. capillacea* in carbon dioxide capturing, sequestration, and utilization in producing various valued and sustainable bioproducts and biofuels, which consequently would help in the climate changes mitigation and preserving the globe temperature rise to less than 2 °C by the end of this century. However, further research is necessary to determine the feasibility and profitability of the proposed blue-based practice. This can be achieved by studying the potential for scaling up, exploring cost-effective harvesting techniques, optimizing the bio-product extraction process, and conducting life cycle assessments to quantify environmental benefits. This is due to several factors that will influence it, including the biomass feedstock's sustainability, plentiful availability, gathering period, and expenses, in addition to its processing, and finally the product's commercialization and compatibility with other existing low-carbon footprint sectors.

Supplementary Information The online version contains supplementary material available at https://doi.org/10.1007/s13762-024-06319-8.

Acknowledgements Authors express their gratitude to the Science, Technology & Innovation Funding Authority (STDF) for funding this work under the grand number 45614.

Author contribution Nour El-Gendy: the corresponding author, put forth the idea of scientific research, conceived and designed research, supervised experimental work, validated the results, interpreted and discussed the results, and wrote the manuscript; Hussein Nassar: Collection and sampling of macroalgae, help in designing and conceiving the research, help in validation, curation, interpretation and discussion of obtained data; Abdallah Ismail: conducting, validating, curating, and discussing the biocidal activity and helped in the performed analysis; Hager Ali and Basma Ali: performed all the extraction and analysis of the value-added products; Khaled Abdelsalam: performed the microscopic identification of macroalgae; Manal Mubarak: performed all proximate, and biochemical analyses of macroalgae All authors have read and agreed to the published version of the manuscript.

Funding Open access funding provided by The Science, Technology & Innovation Funding Authority (STDF) in cooperation with The Egyptian Knowledge Bank (EKB). Science, Technology & Innovation Funding Authority (STDF), 45614.

Data availability Data are available from the corresponding author upon request.

Declarations

Conflicts of interest The authors declare no conflict of interest.

Ethical approval We have followed our ethical norms established by our respective institutions.

References

Abdul Ghani NA, Othaman R, Ahmad A, Anuar FH, Hassan NH (2019) Impact of purification on iota carrageenan as solid polymer electrolyte. Arab J Chem 12:370–376. https://doi.org/10.1016/j.arabjc.2018.06.008

AbouGabal AA, Khaled AA, Aboul-Ela HM, Aly HM, Diab MH, Shalaby OK (2021) Marine macroalgal biodiversity, spatial study for the Egyptian Mediterranean Sea, Alexandria coast. Thalassas:

an Int J Marine Sci 38(1):639–646. https://doi.org/10.1007/s41208-021-00370-9

Abu Hafsa SH, Khalel MS, El-Gindy YM, Hassan AA (2021) Nutritional potential of marine and freshwater algae as dietary supplements for growing rabbits. Ital J Anim Sci 20(1):784–793. https://doi.org/10.1080/1828051X.2021.1928557

Aguiar ALL, Araújo MLH, Benevides NMB, Mattos ALA, Araújo IMS, Silva EMC (2023) Sequential extraction process and physicochemical characterization of R-phycoerythrin and agar from red macroalgae *Gracilaria birdiae*. Algal Res 69:102920. https://doi.org/10.1016/j.algal.2022.102920

Al-Nahdi ZM, Al-Alawi A, Al-Marhobi I (2019) The effect of extraction conditions on chemical and thermal characteristics of kappa-carrageenan extracted from *Hypnea bryoides*. J Mar Biol 2019:5183261. https://doi.org/10.1155/2019/5183261

Al-Sadek AF, Gad BK, Nassar HN, El-Gendy NS (2021) Recruitment of long short-term memory for envisaging the higher heating value of valorized lignocellulosic solid biofuel: a new approach. Energy Sources Part A. https://doi.org/10.1080/15567036.2021.2007179

Al-Saeedi SI, Ashour M, Alprol AE (2023) Adsorption of toxic dye using red seaweeds from synthetic aqueous solution and its application to industrial wastewater effluents. Front Mar Sci 10:1202362. https://doi.org/10.3389/fmars.2023.1202362

Álvarez-Viñas M, Flórez-Fernández N, Torres MD, Domínguez H (2019) Successful approaches for a red seaweed biorefinery. Mar Drugs 17:620. https://doi.org/10.3390/md17110620

Amorim RNS, Rodrigues JAG, Holanda ML, Quinderé ALG, Paula RCM, Melo VMM, Benevides NMB (2012) Antimicrobial effect of a crude sulfated polysaccharide from the red seaweed *Gracilaria ornate*. Braz Arch Biol Techn 55(2):171–181. https://doi.org/10.1590/S1516-89132012000200001

AOAC (2000) Official Methods of Analysis (17th edn) ed. Helrich, K. Arlington, VA: Association of Official Analytical Chemists, Washington DC, USA

Arasamuthu A, Laju RL, Diraviya RK, Kumar TKA, Leewis RJ, Patterson EJK (2023) Invasive red alga *Kappaphycus alvarezii* on the reefs of the Gulf of Mannar, India—a persistent threat to the corals. Bioinvasions Rec 12(1):151–166. https://doi.org/10.3391/bir.2023.12.1.13

Ashour M, El-Shafei AA, Khairy HM, Abd-Elkader DY, Mattar MA, Alataway A, Hassan SM (2020) Effect of *Pterocladia capillacea* seaweed extracts on growth parameters and biochemical constituents of Jew's mallow. Agronomy 10:420. https://doi.org/10.3390/agronomy10030420

ASTM/D5865M. 2019. Standard Test Method for Gross Calorific Value of Coal and Coke

Baghel RS (2023) Developments in seaweed biorefinery research: a comprehensive review. Chem Eng J 454(2):140177. https://doi.org/10.1016/j.cej.2022.140177

Baghel RS, Reddy CRK, Singh RP (2021) Seaweed-based cellulose: applications, and future perspectives. Carbohydr Polym 267:118241. https://doi.org/10.1016/j.carbpol.2021.118241

Beaumont M, Tran R, Vera G, Niedrist D, Rousset A, Pierre R, Shastri VP, Forget A (2021) Hydrogel-forming algae polysaccharides: from seaweed to biomedical applications. Biomacromol 22:1027–1052. https://doi.org/10.1021/acs.biomac.0c01406

Belattmania Z, Bentiss F, Jama C, Nadri A, Reani A, Sabour B (2021) Spectroscopic characterization and gel properties of agar from two Gelidium species from the Atlantic coast of Morocco. Biointerf Res Appl Chem 11(5):12642–12652

Benton JJ (2001) Laboratory Guide for Conducting Soil Test and Plant Analysis; CRC Press: Boca Raton, FL, USA; New York, NY, USA; Washington, DC, USA; London, UK

Bhutiya PL, Misra N, Abdul Rasheed M, Hasan SZ (2020) Silver Nanoparticles deposited algal nanofibrous cellulose sheet for antibacterial activity. BioNanoScience 10:23–33. https://doi.org/10.1007/s12668-019-00690-4

Boo SM, Kim SY, Hong IS, Hwang IL (2010) Reexamination of the genus *Pterocladiella* (Gelidiaceae, Rhodophyta) in Korea based on morphology and rbcL sequences. Algae 25(1):1–9. https://doi.org/10.4490/algae.2010.25.1.001

Bottalico A, Foglie CID, Fanelli M (2008) Growth and reproductive phenology of *Pterocladiella capillacea* (Rhodophyta: Gelidiales) from the southern Adriatic Sea. Bot Mar 51:124–131. https://doi.org/10.1515/BOT.2008.023

Carpena M, Garcia-Perez P, Garcia-Oliveira P, Chamorro F, Otero P, Lourenco-Lopes C, Cao H, Simal-Gandara J, Prieto MA (2023) Biological properties and potential of compounds extracted from red seaweeds. Phytochem Rev 22:1509–1540. https://doi.org/10.1007/s11101-022-09826-z

Castejón N, Parailloux M, Izdebska A, Lobinski R, Fernandes SCM (2021) Valorization of the red algae *Gelidium sesquipedale* by extracting a broad spectrum of minor compounds using green approaches. Mar Drugs 19:574. https://doi.org/10.3390/md19100574

Chapman HD, Pratt PF (1961) Methods of analysis for soils, plants, and waters. University of California, Berkeley, CA, USA, Division of agriculture sciences

Chaudhary J, Thakur S, Sharma M, Gupta VK, Thakur VK (2020) Development of biodegradable agar-agar/gelatin-based superabsorbent hydrogel as an efficient moisture-retaining agent. Biomolecules 10:939. https://doi.org/10.3390/biom10060939

Cherry P, O'Hara C, Magee PJ, McSorley WM, Allsopp PJ (2019) Risks and benefits of consuming edible seaweeds. Nutr Rev 77(5):307–329. https://doi.org/10.1093/nutrit/nuy066

Cichosz S, Masek A (2019) Cellulose fibers hydrophobization via a hybrid chemical modification. Polymers 11:1174. https://doi.org/10.3390/polym11071174

del Río PG, Gomes-Dias JS, Rocha CMR, Romaní A, Garrote G, Domingues L (2020) Recent trends on seaweed fractionation for liquid biofuels production. Biresour Technol 299:122613. https://doi.org/10.1016/j.biortech.2019.122613

Dewi EN, Ibrahim R, Suharto S (2015) Morphological structure characteristic and quality of semi refined carrageenan processed by different drying methods. Procedia Environ Sci 23:116–122. https://doi.org/10.1016/j.proenv.2015.01.018

Ding F, Zhong Y, Wu S, Liu X, Zou X, Li H (2020) Synthesis and characterization of quaternized agar in KOH/urea aqueous solution. New J Chem 44(39):17062–17069

Doh H, Lee MH, Whiteside WS (2020) Physicochemical characteristics of cellulose nanocrystals isolated from seaweed biomass. Food Hydrocoll 102:105542. https://doi.org/10.1016/j.foodhyd.2019.105542

Dorez G, Ferry L, Sonnier R, Taguet A, Lopez-Cuesta J-M (2014) Effect of cellulose, hemicellulose and lignin contents on pyrolysis and combustion of natural fibers. J Anal Appl Pyrolysis 107:323–331. https://doi.org/10.1016/j.jaap.2014.03.017

Eklund B, Svensson AP, Jonsson C, Malm T (2005) Toxic effects of decomposing red algae on littoral organisms. Estuar Coast Shelf Sci 62:621–626. https://doi.org/10.1016/j.ecss.2004.09.030

El Shoubaky GA (2013) Comparison of the impacts of climate change and anthropogenic disturbances on the El Arish coast and seaweed vegetation after ten years in 2010, North Sinai. Egypt Oceanologia 55(3):663–685. https://doi.org/10.5697/oc.55-3.663

El Achaby M, Kassab Z, Aboulkas A, Gaillard C, Barakat A (2018a) Reuse of red algae waste for the production of cellulose nanocrystals and its application in polymer nanocomposites. Int J Biol Macromol 106:681–691. https://doi.org/10.1016/j.ijbiomac.2017.08.067

El Achaby M, Kassab Z, Aboulkas A, Gaillard C, Barakat A (2018b) Reuse of red algae waste for the production of cellulose

nanocrystals and its application in polymer nanocomposites. Int J Biol Macromol 106:681–691. https://doi.org/10.1016/j.ijbiomac.2017.08.067

El-Gendy NSh, Nassar HN, Ismail AR, Ali HR, Ali BA, Abdelsalam KM, Mubarak MA (2023) Fully integrated biorefinery process for the valorization of *Ulva fasciata* into different green and sustainable value-added products. Sustainability 15:7319. https://doi.org/10.3390/su15097319

El-Gendy NS, Hosny M, Ismail AR, Radwan AA, Ali BA, Ali HR, El-Salamony RA, Abdelsalam KM, Mubarak M (2024) A Study on the potential of valorizing *Sargassum latifolium* into biofuels and sustainable value-added products. Int J Biomater 2024(1):5184399

Elnashar MMM, Yassin MA (2009) Lactose hydrolysis by β-galactosidase covalently immobilized to thermally stable biopolymers. Appl Biochem Biotechnol 2009(159):426–437. https://doi.org/10.1007/s12010-008-8453-3

El-Sayed AAM, Ismail MM (2022) Physico-chemodiversity variation between the most common calcareous red seaweed, Eastern Harbor, Alexandria. Egypt Heliyon 8:e12457

European Standard EN15403 (2011), Solid recovered fuels—Determination of ash content

European Standard EN15414. 2011, Solid recovered fuels—Determination of moisture content using the oven dry method—Part 3: Moisture in general analysis sample

Fathy AA, Mohammady NG (2007) Seasonal variation on biomass and agar quality extracted from the marine red algae *Pterocladia capillacea* and *Hypnea musciformis* growing along Mediterranean seashore of Alexandria, Egypt. Egypt J Phycol 8(1):29–38. https://doi.org/10.21608/egyjs.2007.114541

Freile-Pelegrín Y, Robledo D, Armisén R, García-Reina G (1996) Seasonal changes in agar characteristics of two populations of *Pterocladia capillacea* in Gran Canaria. Spain J Appl Phycol 8:239–246. https://doi.org/10.1007/BF02184977

Freitas MV, Pacheco D, Cotas J, Mouga T, Afonso C, Pereira L (2022) Red seaweed pigments from a biotechnological perspective. Phycology 2:1–29. https://doi.org/10.3390/phycology2010001

Gamero-Vega G, Palacios-Palacios M, Quitral V (2020) Nutritional composition and bioactive compounds of red seaweed: a mini-review. J Food Nutr Res 8(8):431–440

Gubelit YI (2022) Opportunistic macroalgae as a component in assessment of eutrophication. Diversity 14(12):1112

Guillén PO, Motti P, Mangelinckx S, De Clerck O, Bossier P, Van Den Hende S (2022) Valorization of the chemical diversity of the tropical red seaweeds *Acanthophora* and *Kappaphycus* and their applications in aquaculture: a review. Front Mar Sci 9:957290. https://doi.org/10.3389/fmars.2022.957290

Guo Y, Lundebye A-K, Li N, Ergon Å, Pang S, Jiang Y, Zhu W, Zhao Y, Li X, Yao L, Wang L, Aakre I (2023) Comparative assessment of food safety regulations and standards for arsenic, cadmium, lead, mercury and iodine in macroalgae used as food and feed in China and Europe. Trends Food Sci Tech 141:104204. https://doi.org/10.1016/j.tifs.2023.104204

Hai LV, Son HN, Seo YB (2015) Physical and bio-composite properties of nanocrystalline cellulose from wood, cotton linters, cattail, and red algae. Cellulose 22:1789–1798. https://doi.org/10.1007/s10570-015-0633-z

Han J, Han X, Xue Z, Wang Q, Xia Y, Zhao Z (2021) An eco-friendly procedure for achieving high-yield carrageenan from *Hypnea cervicornis* suitable for wet spinning. J Appl Polym Sci 138:e50833. https://doi.org/10.1002/app.50833

Han JS, Kim SY, Seo YB (2022) Disk-shaped cellulose fibers from red algae, *Eucheuma cottonii* and its use for high oxygen barrier. Int J Biol Macromol 210:752–758. https://doi.org/10.1016/j.ijbiomac.2022.04.232

Haryatfrehni RH, Dewia SC, Meilianda A, Rahmawati S, Sari IZR (2015) Preliminary study the potency of macroalgae in Yogyakarta: extraction and analysis of algal pigments from common Gunungkidul seaweeds. Procedia Chem 14:373–380. https://doi.org/10.1016/j.proche.2015.03.051

Hassaan MA, El Nemr A, Elkatory MR, Ragab S, El-Nemr MA, Pantaleo A (2021) Synthesis, Characterization, and synergistic effects of modified biochar in combination with α-Fe_2O_3 NPs on biogas production from red algae *Pterocladia capillacea*. Sustainability 13:9275. https://doi.org/10.3390/su13169275

Ibrahim HAH, Beltagy EA, Shams El-Din NG, El Zokm GM, El-Sikaily AM, Abu-Elela GM (2015) Seaweeds agarophytes and associated epiphytic bacteria along Alexandria coastline, Egypt, with emphasis on the evaluation and extraction of agar and agarose. Rev Biol Mar Oceanogr 50(3):545–561. https://doi.org/10.4067/S0718-19572015000400012

Iha C, Jamas M, Guimarães SMPB, Fujii MT, Freshwater DW, Oliveira MC (2017) *Pterocladiella* (Gelidiales, Rhodophyta) species of Brazil including morphological studies of Pterocladiella media and a reassessment of *Pterocladiella taylorii*. Phycologia 56(6):624–637. https://doi.org/10.2216/17-8.1

International organization for standardization (2014). ISO 17225–1. Solid biofuels—Fuel specifications and classes. 56. https://www.iso.org/standard/59456.html

Ismail GA (2016) Biochemical composition of some Egyptian seaweeds with potent nutritive and antioxidant properties. Food Sci Technol 37(2):294–302. https://doi.org/10.1590/1678-457X.20316

Ismail MM, Amer MS (2020) Characterization and biological properties of sulfated polysaccharides of *Corallina officinalis* and *Pterocladia capillacea*. Acta Bot Bras 34(4):623–632. https://doi.org/10.1590/0102-33062020abb0121

Ismail MM, Osman MEH (2016) Seasonal fluctuation of photosynthetic pigments of most common red seaweeds species collected from Abu Qir, Alexandria. Egypt Rev Biol Mar Oceanogr 15(3):515–525. https://doi.org/10.4067/S0718-19572016000300004

Ismail GA, Gheda SF, Abo-Shady AM, Abdel-Karim OH (2020) In vitro potential activity of some seaweeds as antioxidants and inhibitors of diabetic enzymes. Food Sci Technol 40(3):681–691. https://doi.org/10.1590/fst.15619

Jackson ML (1973) Soil Chemical Analysis (2nd ed.), Prentice Hall of India Private Limited, New Delhi, India

Jasem MK, Merai A, Nizam AL (2023) Characterization and in vitro antibacterial activity of sulfated polysaccharides from freshwater alga *Cladophora crispate*. Access Microbiol 5(000537):v5. https://doi.org/10.1099/acmi.0.000537.v5

Javadiyan S, Cooksley CM, Bouras GS, Kao SS-T, Bennett CA, Wormald PJ, Vreugde S, Psaltis AJ (2022) Investigation of kappa carrageenan's muco-adhesive, antibacterial, and anti-biofilm properties. Int Forum Allergy Rhinol 12:302–305. https://doi.org/10.1002/alr.22899

Jmel MA, Messaoud GB, Marzouki MN, Mathlouthi M, Smaali I (2016) Physico-chemical characterization and enzymatic functionalization of *Enteromorpha* sp. cellulose. Carbohydr Polym 135:274–279. https://doi.org/10.1016/j.carbpol.2015.08.048

Johnston KG, Abomohra A, French CE, Zaky AS (2023) Recent advances in seaweed biorefineries and assessment of their potential for carbon capture and storage. Sustainability 15:13193. https://doi.org/10.3390/su151713193

Joniver CFH, Photiades A, Moore PJ, Winters AL, Woolmer A, Adams JMM (2021) The global problem of nuisance macroalgal blooms and pathways to its use in the circular economy. Algal Res 58:102407. https://doi.org/10.1016/j.algal.2021.102407

Jumaah FN, Mobarak NN, Ahmad A, Ghani MA, Rahman MYA (2015) Derivative of iota-carrageenan as solid polymer

electrolyte. Ionics 21:1311–1320. https://doi.org/10.1007/s11581-014-1306-x
Khairy HM, El-Shafay SM (2013) Seasonal variations in the biochemical composition of some common seaweed species from the coast of Abu Qir Bay, Alexandria Egypt. Oceanologia 55(2):435–452. https://doi.org/10.5697/oc.55-2.435
Khairy HM, El-Sheikh MA (2015) Antioxidant activity and mineral composition of three Mediterranean common seaweeds from Abu-Qir Bay. Egypt Saudi J Biol Sci 22(5):623–630. https://doi.org/10.1016/j.sjbs.2015.01.010
Khalafalla MM, El-Hais AMA (2015) Evaluation of seaweeds *Ulva rigida* and *Pterocladia capillaceaas* dietary supplements in Nile tilapia fingerlings. J Aquac Res Development 6:312. https://doi.org/10.4172/2155-9546.100031
Kulal P, Badalamoole V (2020) Hybrid nanocomposite of kappa-carrageenan and magnetite as adsorbent material for water purification. Int J Biol Macromol 165:542–553. https://doi.org/10.1016/j.ijbiomac.2020.09.202
Lai VM-F, Lii C-Y (1998) Effects of extraction conditions on structural and rheological characteristics of agar from *Pterocladia capillacea* and carrageenan from *Grateloupia filicina*. Bot Mar 41:223–234. https://doi.org/10.1515/botm.1998.41.1-6.223
Lai VM-F, Lii C-Y (2002) Gelation kinetics of agars from *Pterocladia capillacea* examined by dynamic rheometry. J Food Sci 67(2):672–681. https://doi.org/10.1515/botm.1998.41.1-6.223
Lakshmi DS, Trivedi N, Reddy CRK (2017) Synthesis and characterization of seaweed cellulose derived carboxymethyl cellulose. Carbohydr Polym 157:1604–1610. https://doi.org/10.1016/j.carbpol.2016.11.042
Lane-Medeiros L, Puppin-Gonçalves CT, Angelini R, Lira AS, Lucena-Frédou F, Freire FAM (2023) Macroalgal blooms affect the food web of tropical coastal ecosystems impacted by fisheries. Mar Environ Res 184:105858. https://doi.org/10.1016/j.marenvres.2022.105858
Lapointe BE, Burkholder JM, Van Alstyne KL (2018) Harmful macroalgal blooms in a changing world: causes, impacts, and management. Harmful Algal Blooms Compend Desk Ref 2:515–560
Lee MW, Han SO, Seo YB (2008) Red algae fibre/poly (butylene succinate) biocomposites: The effect of fibre content on their mechanical and thermal properties. Compos Sci Technol 68:1266–1272. https://doi.org/10.1016/j.compscitech.2007.12.016
Li Z, Cheong K-L, Song B, Yin H, Li Q, Chen J, Wang Z, Xu B, Zhong S (2024) Preparation of κ-carrageenan oligosaccharides by photocatalytic degradation: structural characterization and antioxidant activity. Food Chem X 22:101294. https://doi.org/10.1016/j.fochx.2024.101294
López-Simeon R, Campos-Terán J, Beltrán HI, Hernández-Guerrero M (2012) Free-lignin cellulose obtained from agar industry residues using a continuous and minimal solvent reaction/extraction methodology. RSC Adv 2:12286–12297. https://doi.org/10.1039/c2ra22185c
Lyons DA, Mant RC, Bulleri F, Kotta J, Rilov G, Crow TP (2012) What are the effects of macroalgal blooms on the structure and functioning of marine ecosystems? A Syst Rev Protocol Environ Evid 1:7. https://doi.org/10.1186/2047-2382-1-7
Lyons DA, Arvanitidis C, Blight AJ, Chatzinikolaou E, Guy-Haim T, Kotta J, Orav-Kotta H, Queirós AM, Rilov G, Somerfield PJ, Crowe TP (2014) Macroalgal blooms alter community structure and primary productivity in marine ecosystems. Glob Change Biol 20(9):2712–2724. https://doi.org/10.1016/10.1111/gcb.12644
Machado B, Costa SM, Costa I, Fangueiro R, Ferreira DP (2024) The potential of algae as a source of cellulose and its derivatives for biomedical applications. Cellulose 31:3353–3376. https://doi.org/10.1007/s10570-024-05816-w
Maleki A, Panahzadeh M, Eivazzadeh-keihan R (2019) Agar: a natural and environmentally-friendly support composed of copper oxide nanoparticles for the green synthesis of 1,2,3–triazoles. Green Chem Lett Rev 12(4):395–406. https://doi.org/10.1080/17518253.2019.1679263
Martínez-Sanz M, Gómez-Mascaraque LG, Ballester AR, Martínez-Abad A, Brodkorb A, López-Rubio A (2019) Production of unpurified agar-based extracts from red seaweed *Gelidium sesquipedale* by means of simplified extraction protocols. Algal Res 38:101420. https://doi.org/10.1016/j.algal.2019.101420
Martins A, Pinto FR, Barroso S, Pereira T, Mouga T, Afonso C, Freitas MV, Pinteus S, Pedrosa R, Gil MM (2023) Valorization of the red seaweed *Gracilaria gracilis* through a biorefinery approach. J.vis Exp. https://doi.org/10.3791/65923
Mayhoob H, Abbas A, Mahmod A (2017) Study the effect of agar extraction time on its yield and physical properties of Syrian alga *Pterocladia capillacea*. SSRG Int J Agric Env Sci 4(2):63–65
Mohamed LA, Khaled A (2005) Comparative study of heavy metal distribution in some coastal seaweeds of Alexandria Egypt. Chem Ecol 21(3):181–189. https://doi.org/10.1080/02757540500151614
Mohy El-Din SM, El-Ahwany AMD (2016) Bioactivity and phytochemical constituents of marine red seaweeds (*Jania rubens*, *Corallina mediterranea* and *Pterocladia capillacea*). J Taibah Univ Sci 10(4):471–484. https://doi.org/10.1016/j.jtusci.2015.06.004
Moubasher AH, Hafez SII, Aboelfattah HM, Moharrarh AM (1984) Fungi of wheat and broad bean straw composts. II Thermophilic Fungi Mycopathologia 78(3):169–176. https://doi.org/10.1007/BF00436514
Muthukumar J, Chidambaram R (2022) Isolation and quantification of cellulose from various food grade macroalgal species and its characterization using ATR-FTIR spectroscopy. J Agric Food Res 2(1):1–18
Muthukumar JA, Chidambaram RA (2023) Isolation and quantification of cellulose from various food-grade macroalgal species. Cellulose Chem Technol 57(3–4):237–244
Naduparambath S, Jinitha TV, Shaniba V, Sreejith MP, Balan AK, Purushothaman E (2018) Isolation and characterisation of cellulose nanocrystals from sago seed shells. Carbohydr Polym 180:13–20. https://doi.org/10.1016/j.carbpol.2017.09.088
Nallasivam J, Prashanth PF, Harisankar S, Nori S, Suryanarayan S, Chakravarthy SR, Vinu R (2022) Valorization of red macroalgae biomass via hydrothermal liquefaction using homogeneous catalysts. Bioresour Technol 346:126515. https://doi.org/10.1016/j.biortech.2021.126515
Nassar HN, Rabie AM, Abu Amr SA, El-Gendy NSh (2022) Kinetic and statistical perspectives on the interactive effects of recalcitrant polyaromatic and sulfur heterocyclic compounds and in-vitro nanobioremediation of oily marine sediment at microcosm level. Environ Res 209:112768. https://doi.org/10.1016/j.envres.2022.112768
Nissa RC, Abdullah AHD, Firdiana B, Kosasih W, Endah ES, Marliah S, Rahmat A, Hidayat (2023) Characterization of microcrystalline cellulose from red seaweed *Gracilaria verucosa* and *Eucheuma cottonii*. IOP Conf Ser Earth Environ Sci 1201:012101. https://doi.org/10.1088/1755-1315/1201/1/012101
Offei F, Mensah M, Thygesen A, Kemausuor F (2018) Seaweed bioethanol production: a process selection review on hydrolysis and fermentation. Fermentation 4:99. https://doi.org/10.3390/fermentation4040099
Oprea S (2010) Preparation and characterization of the agar/polyurethane composites. J Compos Mater 45(20):2039–2045. https://doi.org/10.1177/0021998310392415
Osman MEH, Abo-Shady AM, Elshobary ME, Abd El-Ghafar MO, Abomohra A-E (2020) Screening of seaweeds for sustainable

biofuel recovery through sequential biodiesel and bioethanol production. Environ Sci Pollut Res 27:32481–32493. https://doi.org/10.1007/s11356-020-09534-1

Øverland M, Mydland LT, Skrede A (2019) Marine macroalgae as sources of protein and bioactive compounds in feed for monogastric animals. J Sci Food Agric 99(1):13–24. https://doi.org/10.1002/jsfa.9143

Patarra RF, Iha C, Pereira L, Neto AI (2020) Concise review of the species *Pterocladiella capillacea* (S.G. Gmelin) Santelices & Hommersand. J Appl Phycol 32:787–808. https://doi.org/10.1007/s10811-019-02009-y

Perumal P, Selvin PC (2020) Red algae-derived k-carrageenan-based proton-conducting electrolytes for the wearable electrical devices. J Solid State Electr 24:2249–2260. https://doi.org/10.1007/s10008-020-04724-w

Pessarrodona A, Howard J, Pidgeon E, Wernberg T, Filbee-Dexter K (2024) Carbon removal and climate change mitigation by seaweed farming: a state of knowledge review. Sci Total Environ 918:170525. https://doi.org/10.1016/j.scitotenv.2024.170525

Pierre G, Sopena V, Juin C, Mastouri A, Graber M, Maugard T (2011) Antibacterial activity of a sulfated galactan extracted from the marine alga *Chaetomorpha aerea* against *Staphylococcus aureus*. Biotechnol Bioprocess Eng 16:937–945. https://doi.org/10.1007/s12257-011-0224-2

Pino-Ramos VH, Duarte-Peña L, Bucio E (2021) Highly crosslinked agar/acrylic acid hydrogels with antimicrobial properties. Gels 7(4):183. https://doi.org/10.3390/gels7040183

Pradhan B, Ki J-S (2023) Biological activity of algal derived carrageenan: a comprehensive review in light of human health and disease. Int J Biol Macromol 238:124085. https://doi.org/10.1016/j.ijbiomac.2023.124085

Rao AV, Bekheet IA (1976) Preparation of agar-agar from the red seaweed *Pterocladia capillacea* off the coast of Alexandria. Egypt Appl Environ Microbiol 32(4):479–482. https://doi.org/10.1128/aem.32.4.479-482.1976

Rashad S, El-Chaghaby GA (2020) Marine algae in Egypt: distribution, phytochemical composition and biological uses as bioactive resources (a review). Egypt J Aquat Biol Fish 24(5):147–160. https://doi.org/10.21608/ejabf.2020.103630

Rocha CMR, Sousaa AMM, Kim JK, Magalhães JMCS, Yarish C, Gonçalves MP (2019) Characterization of agar from *Gracilaria tikvahiae* cultivated for nutrient bioextraction in open water farms. Food Hydrocoll 89:260–271. https://doi.org/10.1016/j.foodhyd.2018.10.048

Rudke AR, Zanella E, Stambuk BU, Andrade CJ, Ferreira SRS (2024) Deconstruction of *Kappaphycus alvarezii* biomass by pressurized solvents to increase the carrageenan purity. Food Hydrocoll 155:110204. https://doi.org/10.1016/j.foodhyd.2024.110204

Scrosati R (2002) Morphological plasticity and apparent loss of apical dominance following the natural loss of the main apex in *Pterocladiella capillacea* (Rhodophyta, Gelidiales) fronds. Phycologia 41(1):96–98. https://doi.org/10.2216/i0031-8884-41-1-96.1

Sebaaly C, Karaki N, Chahine N, Evidente A, Yassine A, Habib J, Kanaan H (2012) Polysaccharides of the red algae "*Pterocladia*" growing on the Lebanese coast: isolation, structural features with antioxidant and anticoagulant activities. J Appl Pharm Sci 2(10):1–10. https://doi.org/10.7324/JAPS.2012.21001

Serra JP, Salado M, Correia DM, Gonçalves R, del Campo FJ, Lanceros-Mendez S, Costa CM (2023) High-performance sustainable electrochromic devices based on carrageenan solid polymer electrolytes with ionic liquid. ACS Appl Eng Mater 1(5):1416–1425. https://doi.org/10.1021/acsaenm.3c00090

Shams El-Din NG, Shaltout NA, Nassar MZ, Soliman A (2015) Ecological studies of epiphytic microalgae and epiphytic zooplankton on seaweeds of the Eastern Harbor, Alexandria. Egypt Am J Environ Sci 11(6):450–473. https://doi.org/10.3844/ajessp.2015.450.473

Shoaib AGM, El-Sikaily A, El Nemr A, Mohamed AEA, Hassan AA (2022) Preparation and characterization of highly surface area activated carbons followed type IV from marine red alga (*Pterocladia capillacea*) by zinc chloride activation. Biomass Convers Bior 12:2253–2265. https://doi.org/10.1007/s13399-020-00760-8

Siddhanta AK, Prasad K, Meena R, Prasad G, Mehta GK, Chhatbar MU, Oza MD, Kumar S, Sanandiya ND (2009) Profiling of cellulose content in Indian seaweed species. Bioresour Technol 100:6669–6673. https://doi.org/10.1016/j.biortech.2009.07.047

Siddhanta AK, Kumar S, Mehta GK, Chhatbar MU, Oza MD, Sanandiya ND, Chejara DR, Godiya CB, Kondaveeti S (2013) Cellulose contents of some abundant Indian seaweed species. Nat Prod Commun 8(4):497–500. https://doi.org/10.1177/1934578X1300800423

Siller-Sánchez A, Ruiz HA, Aguilar CN, Rodríguez-Jasso RM (2019) Biorefinery approach for red seaweeds biomass as source for enzymes production: Food and biofuels industry. In: Parameswaran B, Varjani S, Raveendran S (eds) Green Bio-processes: enzymes in industrial food processing. Springer Singapore, Singapore, pp 413–446. https://doi.org/10.1007/978-981-13-3263-0_21

Soares F, Fernandes C, Silva P, Pereira L, Gonçalves T (2016) Antifungal activity of carrageenan extracts from the red alga *Chondracanthus teedei* var. *lusitanicus*. J Appl Phycol 28:2991–2998. https://doi.org/10.1007/s10811-016-0849-9

Soliman RM, Younis SA, El-Gendy NSh, Mostafa SSM, El-Temtamy SA, Hashim AI (2018) Batch bioethanol production via the biological and chemical saccharification of some Egyptian marine macroalgae. J Appl Microbiol 125(2):422–440. https://doi.org/10.1111/jam.13886

Souza RB, Frota AF, Silva J, Alves C, Neugebauer AZ, Pinteus C, Rodrigues JAG, Cordeiro EMS, Almeida RR, Pedrosa R, Benevides NMB (2018) In vitro activities of kappa-carrageenan isolated from red marine alga *Hypnea musciformis*: Antimicrobial, anticancer and neuroprotective potential. Int J Biol Macromol 112:1248–1256. https://doi.org/10.1016/j.ijbiomac.2018.02.029

European Standard EN15402 (2011), Solid recovered fuels—Determination of the content of volatile matter

Sultana F, Abdul Wahab M, Nahiduzzaman M, Mohiuddin M, Iqbal MZ, Shakil A, Al Mamun A, Khan MSR, Wong L, Asaduzzaman M (2023) Seaweed farming for food and nutritional security, climate change mitigation and adaptation, and women empowerment: a review. Aquac Fish 8:463–480. https://doi.org/10.1016/j.aaf.2022.09.001

Syaharuddin (2019) Optimization of extraction and quality assessment based on physicochemical properties of carrageenan from red algae (*Kappaphycus alvarezii*) origin of South Sulawesi Indonesia. J Phys Conf Series 1341(7):072013. https://doi.org/10.1088/1742-6596/1341/7/072013

Torres MD, Flórez-Fernández N, Domínguez H (2019) Integral utilization of red seaweed for bioactive production. Mar Drugs 17:314. https://doi.org/10.3390/md17060314

Ulagesan S, Krishnan S, Nam T-J, Choi Y-H (2023) The influence of κ-carrageenan-R-phycoerythrin hydrogel on in vitro wound healing and biological function. Int J Mol Sci 2023(24):12358. https://doi.org/10.3390/ijms241512358

Varma R, Prtihar A, Pasumpon N, Vasudevan S (2022) Extraction and characterisation of cellulose from red seaweeds of *Hypnea musciformis* and *Sarconema filliforme*. Cellulose Chem Technol 56(9–10):949–956

Veeragurunathan V, Prasad K, Malar Vizhi J, Singh N, Meena R, Mantri VA (2019) *Gracilaria debilis* cultivation, agar characterization and economics: bringing new species in the ambit of commercial

farming in India. J Appl Phycol 31:2609–2621. https://doi.org/10.1007/s10811-019-01775-z

Vuai SAH (2022) Characterization of agar extracted from Gracilaria species collected along Tanzanian coast. Heliyon 8:e09002. https://doi.org/10.1016/j.heliyon.2022.e09002

Wahlström N, Harrysson H, Undeland I, Edlund U (2018) A Strategy for the sequential recovery of biomacromolecules from red macroalgae *Porphyra umbilicalis* Kützing. Ind Eng Chem Res 57:42–53. https://doi.org/10.1021/acs.iecr.7b03768

Wahlström N, Edlund U, Pavia H, Toth G, Pell AJ, Jaworski A, Choong FX, Shirani H, Nilsson KPR, RichterDahlfors A (2020) Cellulose from the green macroalgae *Ulva lactuca*: Isolation, characterization, optotracing, and production of cellulose nanofibrils. Cellulose 27:3707–3725. https://doi.org/10.1007/s10570-020-03029-5

Walkley AJ, Black IA (1934) Estimation of soil organic carbon by the chromic acid titration method. Soil Sci 37:29–38

Wang FF, Yao Z, Wu HG, Zhang SX, Zhu NN, Gai X (2012) Antibacterial activities of kappa-carrageenan oligosaccharides. Appl Mech Mater 9(108):194–199

Wang H, Wang G, Gu W (2020a) Macroalgal blooms caused by marine nutrient changes resulting from human activities. J Appl Ecol 57:766–776. https://doi.org/10.1111/1365-2664.13587

Wang X, Yan S, Wang Y, Sun Z, Xia B, Wang G (2020b) Study of the phylogeny and distribution of *Pterocladiella* (Pterocladiaceae, Rhodophyta) from China. Phycologia 59(2):165–176. https://doi.org/10.1080/00318884.2020.1717909

Wassef EA, El-Sayed A-FM, Sakr EM (2013) *Pterocladia* (Rhodophyta) and *Ulva* (Chlorophyta) as feed supplements for European seabass, *Dicentrarchus labrax* L., fry. J Appl Phycol 25:1369–1376. https://doi.org/10.1007/s10811-013-9995-5

Watanabe FS, Olsen SR (1965) Test of an ascorbic acid method for determining phosphorus in water and $NaHCO_3$ extracts from the soil. Soil Sci Soc Am J 29:677–678. https://doi.org/10.2136/sssaj1965.03615995002900060025x

Winarni I, Santoso J, Wibowo T (2022) Bioethanol production from seaweed solid waste biomass of agar processing. IOP Conf Ser: Earth Environ Sci. https://doi.org/10.1088/1755-1315/1027/1/012029

Wu C-H, Chien W-C, Chou H-K, Yang J, Lin H-TV (2014) Sulfuric acid hydrolysis and detoxification of red alga *Pterocladiella capillacea* for bioethanol fermentation with thermotolerant yeast *Kluyveromyces marxianus*. J Microbiol Biotechnol 24(9):1245–1253. https://doi.org/10.4014/jmb.1402.02038

Xiao Q, Wang X, Zhang J, Zhang Y, Chen J, Chen F, Xiao A (2021) Pretreatment Techniques and green extraction technologies for agar from *Gracilaria lemaneiformis*. Mar Drugs 19:617. https://doi.org/10.3390/md19110617

Young CS, Lee C-S, Sylvers LH, Venkatesan AK, Gobler CJ (2022) The invasive red seaweed, *Dasysiphonia japonica*, forms harmful algal blooms: mortality in early life stage fish and bivalves and identification of putative toxins. Harmful Algae 118:102294. https://doi.org/10.1016/j.hal.2022.102294

Yousef NS, Salem RH, Abo Zaid EM, El-kader A (2015) Enriching balady bread using red algae (*Pterocladia capillacea*). Egypt J Agricult Sci 66(3):234–244

Zhang R, Wang W, Zhang H, Dai Y, Dong H, Hou H (2019) Effects of hydrophobic agents on the physicochemical properties of edible agar/maltodextrin films. Food Hydrocoll 88:283–290. https://doi.org/10.1016/j.foodhyd.2018.10.008

Zhou F, Liu P, Liu Q, Jin X-H, Xiong X-Y, Zheng Z-J, Ouyang J (2022) Extending galactose-oxidation pathway of Pseudomonas putida for utilization of galactose-rich red macroalgae as sustainable feedstock. J Biotechnol 348:1–9. https://doi.org/10.1016/j.jbiotec.2022.02.009